Monthly Notices
of the
ROYAL ASTRONOMICAL SOCIETY

Mon. Not. R. Astron. Soc. **413,** 921–941 (2011) doi:10.1111/j.1365-2966.2010.18182.x

The evolution of early-type galaxies in clusters from $z \sim 0.8$ to $z \sim 0$: the ellipticity distribution and the morphological mix

Benedetta Vulcani,[1,2]★† Bianca M. Poggianti,[2] Alan Dressler,[3] Giovanni Fasano,[2] Tiziano Valentinuzzi,[1] Warrick Couch,[4] Alessia Moretti,[2] Luc Simard,[5] Vandana Desai,[6] Daniela Bettoni,[2] Mauro D'Onofrio,[1] Antonio Cava[7,8] and Jesús Varela[2]

[1]*Astronomical Department, Padova University, Italy*
[2]*INAF-Astronomical Observatory of Padova, Italy*
[3]*The Observatories of Carnegie Institution of Washington, 813 Santa Barbara Street, Pasadena, CA 91101, USA*
[4]*School of Physics, University of New South Wales, Sydney, Australia*
[5]*National Research Council of Canada, Herzberg Institute of Astrophysics, Victoria, British Columbia V9E 2E7, Canada*
[6]*Spitzer Science Center, California Institute of Technology, 1200 E California Blvd, Pasadena, CA 91125, USA*
[7]*Instituto de Astrofisica de Canarias, Spain*
[8]*Departamento de Astrofisica, Universidad de La Laguna, Spain*

Accepted 2010 December 10. Received 2010 December 9; in original form 2010 October 18

ABSTRACT

We present the ellipticity distribution and its evolution for early-type galaxies in clusters from $z \sim 0.8$ to the current epoch, based on the WIde-field Nearby Galaxy-cluster Survey ($0.04 \leq z \leq 0.07$) and the ESO Distant Cluster Survey ($0.4 \leq z \leq 0.8$). We first investigate a mass-limited sample and we find that above a fixed mass limit ($M_* \geq 10^{10.2}\,M_\odot$), the ellipticity ($\epsilon$) distribution of early-type galaxies notably evolves with redshift. In the local Universe, there are proportionally more galaxies with higher ellipticity, hence flatter, than in distant clusters. This evolution is due partly to the change in the mass distribution and mainly to the change in the morphological mix with z among the early types, the fraction of ellipticals goes from ∼70 per cent at high z to ∼40 per cent at low z). Analysing separately the ellipticity distribution of the different morphological types, we find no evolution both for ellipticals and for S0s. However, for ellipticals a change with redshift in the median value of the distributions is detected. This is due to a larger population of very round ($\epsilon < 0.05$) elliptical galaxies at low z. In order to compare our finding to previous studies, we also assemble a magnitude-'delimited' sample that consists of early-type galaxies on the red sequence with $-19.3 > M_B + 1.208z > -21$. Analysing this sample, we do not recover exactly the same results as the mass-limited sample. This indicates that the selection criteria are crucial to characterize the galactic properties: the choice of the magnitude-'delimited' sample implies the loss of many less-massive galaxies and so it biases the final conclusions. Moreover, although we are adopting the same selection criteria, our results in the magnitude-'delimited' sample are also not in agreement with those of Holden et al. This is due to the fact that our and their low-$z$samples have a different magnitude distribution because the Holden et al. sample suffers from incompleteness at faint magnitudes.

Key words: galaxies: clusters: general – galaxies: elliptical and lenticular, cD – galaxies: evolution – galaxies: formation – galaxies: structure.

1 INTRODUCTION

Ellipticals and lenticulars (S0s) belong to the class of early-type galaxies. This means that they have several properties in common: they dominate the total galaxy population at high masses, they preferentially inhabit dense regions of the universe, such as rich

★E-mail: benedetta.vulcani@oapd.inaf.it
†Visiting The Observatories of Carnegie Institution of Washington, Pasadena, CA, USA.

clusters (Dressler et al. 1997), they tend to be passive, they have red colours and their spectra show strong values of the characteristic *D*4000 feature (see e.g. Kauffmann et al. 2003; Brinchmann et al. 2004), they lack spiral arms and in most cases they exhibit neither major dust features nor a large interstellar gas content. For these reasons, they are often considered together.

On the other hand, elliptical and S0 galaxies differ in several important ways: S0s are bulge-dominated systems with an identifiable disc (e.g. Scorza & van den Bosch 1998; Laurikainen et al. 2007) that is mainly rotationally supported (e.g. Erwin et al. 2003; Cappellari et al. 2005), their intrinsic shape is similar to that of spirals (Rood & Baum 1967; Sandage, Freeman & Stokes 1970) and their formation is still not well understood. Hubble (1936) first proposed their existence as a transitional class between ellipticals and spirals. Understanding how they form and evolve is essential if we wish to have a complete picture of how the galaxy morphology is related to the galaxy formation and the environment.

Then again ellipticals show ellipsoidal shapes, not rarely with significant kinematic twists, and kinematically decoupled components in their centres. Most of them are not characterized by strong rotation (Bertola & Capaccioli 1975) and their luminosity profiles follow a Sérsic law. In the local Universe, discy ellipticals are probably the high bulge mass end of S0 galaxies.

Morphologically, Dressler et al. (1997) showed that, at least for bright galaxies, the raising fraction of early-type galaxies since $z \sim 0.5$ corresponds mainly to an increase in lenticular S0 galaxies, with a roughly constant elliptical fraction. S0s are quite rare in clusters at high redshift ($z > 0.3$–0.4); as a consequence, they have to acquire their shapes with different time-scales and later than ellipticals. The evolving fraction of S0s in clusters might result from the evolving population of newly accreted spiral galaxies from infalling groups and the field.

Fasano et al. (2000) showed that the cluster S0-to-elliptical ratio is, on average, a factor of $\sim$5 higher at $z \sim 0$ than at $z \sim 0.5$. At higher redshift, there is no evidence for any further evolution of the S0 fraction in clusters to $z \sim 1$: most of the evolution occurs since $z \sim 0.4$ (see e.g. Postman et al. 2005; Desai et al. 2007; Wilman et al. 2009).

Dressler et al. (1997) and Postman et al. (2005) also investigated the ellipticity distributions of the S0 and elliptical galaxies in their magnitude-limited samples. They found that the ellipticity distribution of S0 and elliptical galaxies shows no evolution over the broad redshift ranges in their samples. Moreover, they differ from each other, providing evidence for the existence of two distinct classes of galaxies.

In contrast, in their magnitude-'delimited' sample (with both an upper and a lower magnitude limit), Holden et al. (2009) found no evolution in neither the median ellipticity nor the shape of the ellipticity distribution with redshift for early-type (ellipticals + S0s) red-sequence galaxies. This led them to conclude that there has been little or no evolution in the overall distribution of the bulge-to-disc ratio of early-type galaxies from $z \sim 1$ to $z \sim 0$. Assuming that the intrinsic ellipticity distribution of both elliptical and S0 galaxies separately remains constant, they finally concluded that the relative fractions of ellipticals and S0s do not evolve from $z \sim 1$ to $z = 0$ for a red-sequence-selected sample of galaxies.

All the cited works analysed samples limited in some ways by magnitude cuts. For the first time, in this paper, we analyse the evolution of the ellipticity distribution of early-type galaxies also in a mass-limited sample. For the sample in the local Universe, we analyse the data of the WIde-field Nearby Galaxy-cluster Survey (WINGS) (Fasano et al. 2006), while for that in the distant Universe, we use the ESO Distant Cluster Survey (EDisCS) (White et al. 2005). These large cluster samples and their high quality images (see Section 2) allow us to properly characterize the cluster environment at the two redshifts and to subdivide galaxies into the different morphological types and obtain robust estimates of the ellipticity.

This paper is organized as follows. In Section 2, we present the cluster and galaxy samples [WINGS (Fasano et al. 2006) and EDisCS (White et al. 2005)], describing the surveys, the data reduction, and the determination of morphologies, ellipticites and masses. We also depict the selection criteria we follow to assemble the mass-limited and the magnitude-'delimited' samples. In Section 3, we show the results of our analysis of the evolution of the ellipticity distribution with redshift in our mass-limited samples, while in Section 4, we show the same for the magnitude-'delimited' samples. In Section 5, we try to reconcile the results of the different samples, while in Section 6, we compare our results with those found in the literature (in particular with the results drawn by Holden et al. 2009). Finally, in Section 7, we discuss and summarize our findings.

Throughout this paper, we assume $H_0 = 70\,\mathrm{km\,s^{-1}\,Mpc^{-1}}$, $\Omega_\mathrm{m} = 0.30$ and $\Omega_\Lambda = 0.70$. The adopted initial mass function (IMF) is a Kroupa (2001) one in the mass range 0.1–100 $\mathrm{M}_\odot$.

2 CLUSTER AND GALAXY SAMPLES

To perform the study of the ellipticity ($\epsilon \equiv 1 - b/a$, $b \equiv$ semiminor axis, $a \equiv$ semimajor axis) distribution and its evolution from $z \sim 0.8$ to $z \sim 0$ for early-type galaxies and for ellipticals and S0s separately, we assemble two different galaxy cluster samples in two redshift intervals: we draw the samples at low z from the WINGS (Fasano et al. 2006) and those at high z from the EDisCS (White et al. 2005).

First of all, we use a mass-limited sample, that ensures completeness, that is, includes all galaxies more massive than the limit, regardless of their colour or morphological type. We think that this is the best choice to properly characterize galaxy properties.

Then, since Holden et al. (2009) have already analysed the ellipticity distribution using a sample delimited in magnitude both at faint and at bright magnitudes, in order to compare our results with theirs, we also assemble a magnitude-'delimited' sample, following their selection criteria.

2.1 Low-z sample: WINGS

The main goal of the WINGS[1] (Fasano et al. 2006), a multiwavelength survey of clusters at $0.04 < z < 0.07$, is to characterize the photometric and spectroscopic properties of galaxies in nearby clusters and to describe the changes in these properties depending on the galaxy mass and environment. The project was based on deep optical (B, V) wide-field images of 77 fields (Varela et al. 2009) centred on nearby clusters of galaxies selected from three X-ray-flux-limited samples compiled from *ROSAT* All-Sky Survey data (Ebeling et al. 1998, 2000) and the X-ray Brightest Abell-type Cluster sample (Ebeling et al. 1996).

WINGS clusters cover a wide range of velocity dispersion σ_clus (typically 500–1100 $\mathrm{km\,s^{-1}}$) and a wide range of X-ray luminosity L_X [typically $(0.2\text{–}5) \times 10^{44}\,\mathrm{erg\,s^{-1}}$].

The survey has been complemented by a near-infrared (near-IR) (J, K) survey of a subsample of 28 clusters, obtained with the WFCAM@UKIRT (Valentinuzzi et al. 2009), by a spectroscopic

[1] http://web.oapd.inaf.it/wings

survey of a subsample of 48 clusters, obtained with the spectrographs WYFFOS@WHT and 2dF@AAT (Cava et al. 2009) and by *U* broad-band and Hα narrow-band imaging of a subset of WINGS clusters, obtained with wide-field cameras at different telescopes (INT, LBT, Bok) (Omizzolo et al., in preparation).

The spectroscopic target selection was based on the WINGS (B, V) photometry. The aim of the target selection strategy was to maximize the chances of observing galaxies at the cluster redshift without biasing the cluster sample. Galaxies with a total $V \leq 20$ mag, a V magnitude within the fibre aperture of $V < 21.5$ and with a colour within a 5-kpc aperture of $(B - V)_{5\,\mathrm{kpc}} \leq 1.4$ were selected, to reject background galaxies. The exact cut in colour was varied slightly from cluster to cluster in order to account for the redshift variation and to optimize the observational setup. These very loose selection limits were applied so as to avoid any bias in the colours of selected galaxies.

Our optical imaging covers a 34×34-arcmin^2 field. This imaging corresponds to about $0.6R_{200}$ or more, for most clusters, although in a few cases only $\sim 0.5R_{200}$ is covered. R_{200} is defined as the radius delimiting a sphere with the interior mean density 200 times the critical density of the Universe at that redshift and is commonly used as an approximation for the cluster virial radius. The R_{200} values for our structures are computed from the velocity dispersions by Cava et al. (2009).

2.1.1 *Morphologies*

Morphological types are derived from V-band images using MORPHOT, an automatic tool for galaxy morphology, purposely devised in the framework of the WINGS project. MORPHOT was designed with the aim to reproduce as closely as possible visual morphological classifications.

MORPHOT extends the classical Concentration/Asymmetry/clumpinesS (CAS) parameter set (Conselice 2003) by using 20 image-based morphological diagnostics. 14 of them have never been used, while the remaining six [the CAS parameters, the Sérsic index, the Gini and M20 coefficients (Lotz, Primack & Madau 2004)] are already present in the literature, although in slightly different forms. An exhaustive description of MORPHOT will be given in a forthcoming paper (Fasano et al., in preparation), where also the morphological catalogues of the WINGS clusters will be presented and discussed. Provisionally, we refer the reader to Fasano et al. (2007) and Fasano et al. (2010, appendix A therein) for an outlining of the logical sequence and the basic procedures of MORPHOT. Here we just mention that, among the 14 newly devised diagnostics, the most-effective one in order to disentangle ellipticals from S0 galaxies turned out to be an Azimuthal coefficient, measuring the correlation between azimuth and pixel flux relative to the average flux value of the elliptical isophote passing through the pixel itself. From Vulcani et al. (2010a), we report here in Fig. 1 a plot illustrating the capability of the distributions of the Azimuthal coefficient in disentangling elliptical from S0 galaxies, a crucial point in the present analysis.

More importantly for our purposes, the quantitative discrepancy between automatic (MORPHOT) and visual classifications turns out to be similar to the typical discrepancy among visual classifications given by experienced, independent human classifiers (rms $\sim$ 1.3–2.3 T types). The last one has been estimated from a sample of 233 SDSS galaxies included in the Third Reference Catalog of Bright Galaxies (RC3, de Vaucouleurs et al. 1991), whose visual classification was carried out independently by GF and AD and also compared with that given in the RC3. The comparison between the visual (GF) and automatic (MORPHOT) classification is illustrated in

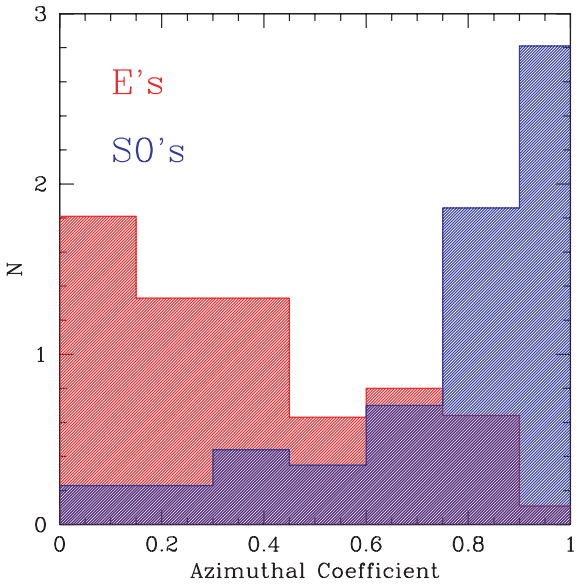

Figure 1. Normalized distributions of the MORPHOT Azimuthal coefficient for the visually classified ellipticals (366 objects, red histogram) and S0 galaxies (267 objects, blue histogram) of the MORPHOT calibration sample. The Azimuthal coefficient measures the correlation between azimuth and pixel flux relative to the average flux value of the elliptical isophote passing through the pixel itself (from Vulcani et al. 2010a).

Fig. 2 for the MORPHOT calibration sample (931 galaxies). In this figure (from Vulcani et al. 2010a), the automatic classification is also shown to be bias-free in the overall range of morphological types, perhaps apart from the last bin, that is, that relative to the very late and irregular galaxies.

For now, we can apply MORPHOT just to the WINGS imaging, because the tool is calibrated on the WINGS imaging characteristics and we defer to a later time a more generally usable version of the

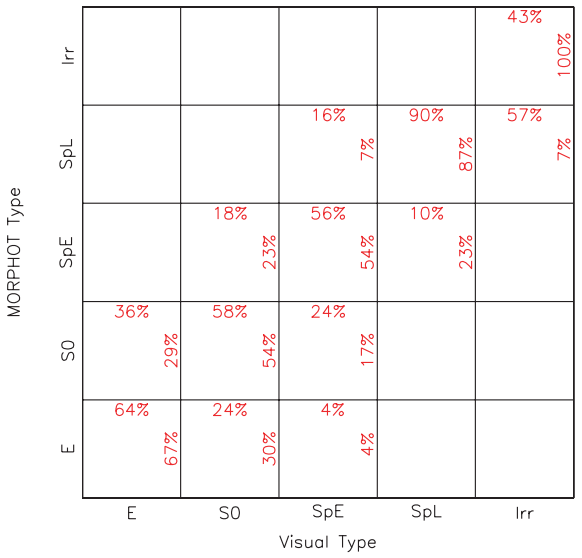

Figure 2. Comparison between visual and MORPHOT broad morphological types for the 931 galaxies of the MORPHOT calibration sample. In each one of the 2D bins of the plot, the percentages of the visual broad types (ellipticals, S0s, early spirals [SpE], late spirals [SpL] and irregulars) falling in different bins of the MORPHOT (broad) classification are reported on the top. Similarly, on the right-hand side of each bin, the percentages of MORPHOT types falling in different bins of the visual types are reported.

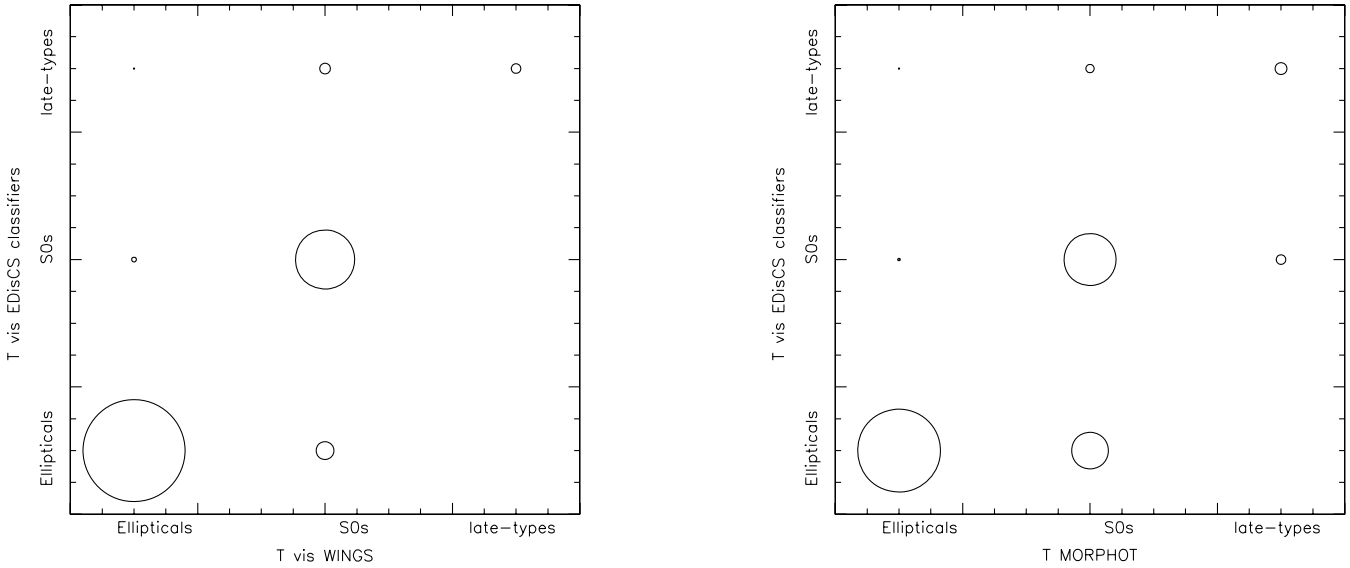

Figure 3. Comparison between the visual classification performed by the EDisCS classifiers and the WINGS visual classification (left-hand panel) and the automatic classification performed by MORPHOT (right-hand panel). The circle radius is proportional to the number of galaxies.

tool. In the following, for the EDisCS imaging, we will use visual morphological classifications. To directly verify that the two methods adopted at different redshifts (see Section 2.2) are consistent, we can apply the same 'method' (visual classification and persons) that was used at high z on the low-z images.

To this aim, three of the classifiers that in 2007 visually classified all the EDisCS galaxies (BMP, AAS, VD) now performed a visual classification of WINGS galaxies. This was done on the subset of WINGS galaxies that was used to calibrate MORPHOT on the visual WINGS morphologies, including only galaxies that enter the sample we analyse in this paper (173 galaxies).

The results (see Fig. 3 taken from Vulcani et al. 2010a) show an agreement between the three broad morphological classes assigned by the EDisCS classifiers with the WINGS visual classification in ∼83 per cent of the cases and with MORPHOT in ∼75 per cent of the cases. Again, these discrepancies turn out to be similar to the typical discrepancy among visual classifications given by experienced, independent human classifiers, so we conclude that the different methods adopted provide a comparable classification.

2.1.2 *Ellipticity measurements*

Galaxy ellipticities have been computed using the tool GASPHOT (Pignatelli, Fasano & Cassata 2006). This is heavily based on the SExtractor ('Source Extractor') galaxy photometry package (Bertin & Arnouts 1996) and provides, among other quantities, ellipticity profiles of galaxies extracted from CCD frames. It fits simultaneously the major and minor axis light growth curves of galaxies with a 2D flattened Sérsic law, convolved by the appropriate, space-varying point spread function (PSF), which was previously evaluated by the tool itself using the stars present in the frame. This approach exploits the robustness of the 1D fitting technique, saving at the same time the capability, typical of 2D approaches, of dealing with the PSF convolution of flattened galaxies. The tool was previously tested for non-Sérsic profiles and blended objects and its results compared with other tools, such as GALFIT (Peng et al. 2002) and GIM2D (Galaxy IMage 2D) (Marleau & Simard 1998), as shown in Pignatelli et al. (2006).

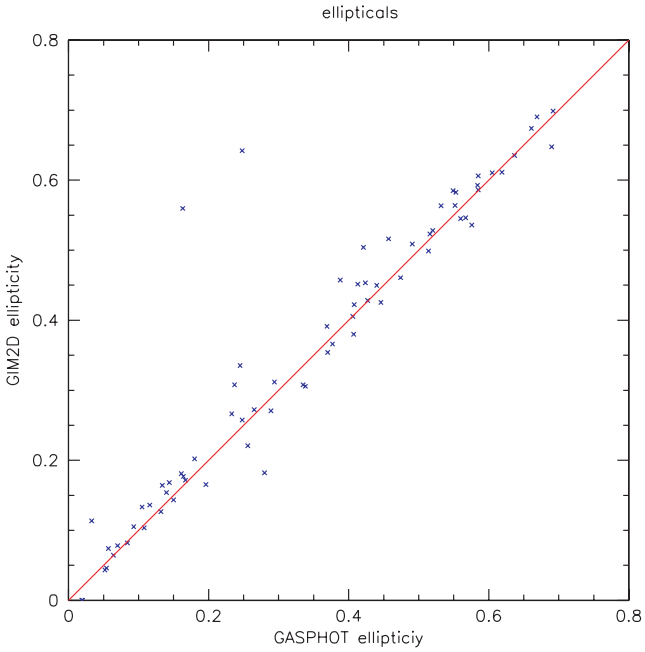

Figure 4. Comparison between the ellipticity estimation from GASPHOT and GIM2D for early-type galaxies of the cluster A119.

Since in our analysis we are comparing the ellipticities of WINGS galaxies to those of EDisCS galaxies, that have been determined using the tool GIM2D (see Section 2.2), we also performed a comparison between the values estimated by the two different tools for early-types galaxies in the WINGS cluster A119. As shown in Fig. 4, the estimates are in good agreement (rms ∼ 0.07).

2.1.3 *Galaxy stellar masses*

Stellar masses have been determined using the relation between the mass-to-light ratio (M/L_B) and rest-frame ($B-V$) colour, following Bell & de Jong (2001) who used a spectrophotometric model finding a strong correlation between the M/L and optical colours of the

integrated stellar populations for a wide range of star formation histories. This method was chosen to be consistent with that adopted for galaxy masses at high z and because it can be used also for galaxies with no spectroscopy in the magnitude-'delimited' sample.

We use the equation that Bell & de Jong (2001) give for the Bruzual & Charlot model with a Salpeter (1955) IMF (0.1–125 $M_\odot$) and solar metallicity:

$$\log_{10}(M/L_B) = -0.51 + 1.45 \times (B - V). \quad (1)$$

The total luminosity L_B has been derived from the total (SExtractor AUTO) observed B magnitude (Varela et al. 2009), corrected for the distance modulus and foreground Galaxy extinction, and k-corrected using tabulated values from Poggianti (1997). The $(B - V)$ colour used to calculate masses was derived from observed B and V aperture magnitudes measured within a diameter of 10 kpc around each galaxy baricentre, corrected as the total magnitude.

Then, we scaled our masses to the more used Kroupa (2001) IMF adding −0.19 dex to the logarithmic value of the masses.

Stellar masses for WINGS galaxies observed spectroscopically had been previously determined by fitting the optical spectrum (in the range ∼3600 to ∼7000 Å) (Fritz et al. 2010), with the spectrophotometric model fully described in Fritz et al. (2007), and they are in good agreement with the masses used in this paper. For a detailed description of the determination of masses and a comparison of different methods, see Fritz et al. (2010), fig. 1 in Vulcani et al. (2010a) and Valentinuzzi et al. (2010).

2.1.4 *Mass-limited sample*

For the mass-limited sample, we rely on spectroscopy to be sure that we are using only cluster members. In the WINGS, photo-z techniques cannot be used to assess the cluster membership due to the low redshift and due to the fact the we have at our disposal few photometric bands. Galaxies are considered members of a cluster if their spectroscopic redshift lies within $\pm 3\sigma$ from the cluster mean redshift, where σ is the cluster velocity dispersion (Cava et al. 2009). We use only spectroscopically confirmed members of 21 of the 48 clusters. The clusters used in this analysis are listed in Table 1. This is the subset of clusters that have a spectroscopic completeness (the ratio of the number of spectra yielding a redshift to the total number of galaxies in the photometric catalogue) larger than 50 per cent. We apply a statistical correction to correct for incompleteness, weighting each galaxy by the inverse of the ratio of the number of spectra yielding a redshift to the total number of galaxies in the V-band photometric catalogue, in bins of 1 mag (Cava et al. 2009).

In each cluster, we exclude the brightest cluster galaxy (BCG), defined as the most-luminous galaxy of each cluster, that has peculiar properties and could alter the distributions (Fasano et al. 2010).

Only galaxies lying within $0.6R_{200}$ are considered, because this is the largest radius covered in the 21 clusters considered (except for A1644 and A3266 where the coverage extends to $\sim 0.5R_{200}$).

To determine the galaxy stellar mass limit of our sample, we compute the mass of an object whose observed magnitude is equal to the faint magnitude limit of the survey and whose colour is the reddest colour of a galaxy at the highest redshift considered.

The spectroscopic magnitude limit of the WINGS is $V = 20$. Considering the distance module of the most-distant WINGS cluster is ∼37.5 and the reddest galaxy has a colour of $(B - V) = 1.2$, the magnitude limit corresponds to a mass limit $M_* = 10^{9.8}\,M_\odot$, above which the sample is unbiased. Adopting this limit, the final sample consists of 951 early-type galaxies, of which 364 are ellipticals and 587 are S0s. The corresponding numbers weighted for incompleteness are 1469 early types, 557 ellipticals and 912 S0s. The numbers of WINGS galaxies above the EDisCS mass limit ($M_* = 10^{10.2}\,M_\odot$, see below) are 594 early types (920 once weighted), 224 ellipticals (341 once weighted) and 370 S0s (579 once weighted) (see Table 2).

Table 1. List of WINGS clusters analysed in the mass-limited sample, their redshift, velocity dispersion, distance modulus (DM) and R_{200}.

Cluster name	z	σ (km s^{-1})	DM (mag)	R_{200} (kpc)
A1069	0.0653	690 ± 68	37.34	1.65
A119	0.0444	862 ± 52	36.47	2.09
A151	0.0532	760 ± 55	36.87	1.83
A500	0.0678	658 ± 48	37.42	1.58
A754	0.0547	1000 ± 48	36.94	2.41
A957x	0.0451	710 ± 53	36.50	1.72
A970	0.0591	764 ± 47	37.11	1.84
A1631a	0.0461	640 ± 33	36.55	1.55
A1644	0.0467	1080 ± 54	36.58	2.61
A2382	0.0641	888 ± 54	37.30	2.13
A2399	0.0578	712 ± 41	37.06	1.71
A2415	0.0575	696 ± 51	37.05	1.67
A3128	0.06	883 ± 41	37.15	2.12
A3158	0.0593	1086 ± 48	37.12	2.61
A3266	0.0593	1368 ± 60	36.12	3.29
A3376	0.0461	779 ± 49	36.55	1.88
A3395	0.05	790 ± 42	36.73	1.91
A3490	0.0688	694 ± 52	37.46	1.66
A3556	0.0479	558 ± 37	36.64	1.35
A3560	0.0489	710 ± 41	36.68	1.72
A3809	0.0627	563 ± 40	37.25	1.35

2.1.5 *Magnitude-'delimited' sample*

For the magnitude-'delimited' sample, we use the photometric data for 76 WINGS clusters.[2] The clusters used are those presented in Table 1 plus those in Table 3.

We follow the selection criteria proposed by Holden et al. (2009). They selected a sample of early-type galaxies (ellipticals and S0s) that lie on the red sequence (determined with spectroscopic members and accepting all galaxies lying within 2σ from the sequence – for details see Mei et al. 2009). At low z, they used only spectroscopically confirmed members. At high z, they considered all red-sequence galaxies in the photometric catalogue except those that are interlopers confirmed by spectroscopy. Moreover, they selected galaxies within a magnitude range, taking into account passive evolution: $-19.3 > M_B + 1.208z > -21$. Finally, they considered only galaxies within $2R_{200}/\pi$ of the cluster centre. They computed ellipticities using the results from GALFIT (Peng et al. 2002) and adopted visual morphologies from the literature (Dressler 1980 for the sample at low z, Desai et al. 2007 and Postman et al. 2005 for the sample at high z).

For our WINGS magnitude-'delimited' sample, to be strictly consistent with what we do for the EDisCS data set, we consider all galaxies in the photometric catalogue, excluding those that are non-members based on the spectroscopy. Contamination on the

[2] A3562 was excluded due to bad V-band seeing.

Table 2. Number of galaxies in the mass-limited and in the magnitude-'delimited' samples. For the mass-limited sample, for WINGS, both the observed numbers and the numbers weighted for the spectroscopic incompleteness are given.

	WINGS					EDisCS	
	$M_* \geq 10^{9.8}\,M_\odot$		$M_* \geq 10^{10.2}\,M_\odot$		mag	$M_* \geq 10^{10.2}\,M_\odot$	mag
	N_{obs}	N_w	N_{obs}	N_w	N	N	N
Ellipticals	364	557	224	341	580	145	101
S0s	587	912	370	579	914	61	43
Early types	951	1469	594	920	1494	206	144

red sequence at low z is minimal and we have checked that the results remain the same using only spectroscopic members corrected for completeness. We exclude from our analysis galaxies located outside R_{200}, to be consistent with what we do at high z (see Section 2.2.2).

We then select only galaxies lying within 2σ from the red sequence. Like Mei et al. (2009), we define the red sequence using only spectroscopic members and we build a colour–magnitude diagram for each cluster. To do this, we use the observed B and V aperture magnitude measured within a diameter of 5 kpc around each galaxy baricentre and the total V SExtractor AUTO magnitude, both corrected for the distance modulus and foreground Galaxy extinction, and k-corrected using tabulated values from Poggianti (1997). For those clusters for which spectroscopy was not available, we define the red sequence using the photometry of morphologically selected early-type galaxies. We determine the slope and the dispersion of the red sequence in the colour–magnitude diagram by performing a weighted least-squares fit on the data, giving less weight to the outliers and reiterating 10 times to have a better determination of the parameters.

We include galaxies with $-19.3 > M_B + 1.208z > -21$, where M_B is the magnitude derived from the total (SExtractor AUTO) observed B magnitude (Varela et al. 2009), corrected as the colour. In this way, we automatically exclude the BCGs. Finally, we consider only galaxies that are ellipticals and S0s, following our morphological classification.

Our final magnitude-'delimited' sample consists of 580 ellipticals and 914 S0s, for a total of 1494 early-type galaxies (see Table 2).

2.2 High-z sample: EDisCS

The multiwavelength photometric and spectroscopic survey of distant clusters, named the EDisCS (White et al. 2005), has been developed to characterize both the clusters themselves and the galaxies within them. It observed 20 fields containing galaxy clusters at $0.4 < z < 1$.

Clusters were drawn from the Las Campanas Distant Cluster Survey catalogue (Gonzalez et al. 2001). They were selected as surface brightness peaks in smoothed images taken with a very wide optical filter (∼4500–7500 Å). The 20 EDisCS fields were chosen from among the 30 highest surface brightness candidates, after confirmation of the presence of an apparent cluster and of a possible red sequence with VLT 20-min exposures in two filters (White et al. 2005).

For all 20 fields, the EDisCS has obtained deep optical multiband photometry with the FORS2/VLT (White et al. 2005) and near-IR photometry with the SofI/NTT (Aragón-Salamanca et al., in preparation). Photometric redshifts were measured using both optical and IR imaging (see Pelló et al. 2009; Rudnick et al. 2009 for details). They were computed for every object in the EDisCS fields using two independent codes, a modified version of the publicly available HYPERZ code (Bolzonella, Miralles & Pelló 2000) and the code of Rudnick et al. (2001) with the modifications presented in Rudnick et al. (2003). Photo-z membership (see also De Lucia et al. 2004, 2007 for details) was established using a modified version of the technique first developed in Brunner & Lubin (2000), in which the probability of a galaxy to be at redshift z [$P(z)$] is integrated in a slice around the cluster redshift to give P_{clust} for the two codes. A galaxy was rejected from the membership list if P_{clust} was smaller than a certain probability P_{thresh} for either code. The P_{thresh} value for each cluster was calibrated from EDisCS spectroscopic redshifts and was chosen to maximize the efficiency with which spectroscopic non-members are rejected while retaining at least ∼90 per cent of the confirmed cluster members, independent of their rest-frame ($B - V$) colour or observed ($V - I$) colour. In practice, it was possible to choose thresholds such that this criterion was satisfied while rejecting 45–70 per cent of spectroscopically confirmed non-members. Applied to the entire magnitude-limited sample, these thresholds reject 75–93 per cent of all galaxies with $I_{tot} < 24.9$. A posteriori, it was verified that in the sample of galaxies with spectroscopic redshift and above the mass limit described below, 20 per cent of those galaxies that are photo-z cluster members are spectroscopically interlopers and, conversely, only 6 per cent of those galaxies that are spectroscopic cluster members are rejected by the photo-z technique.

Deep spectroscopy with the FORS2/VLT was obtained for 18 of the fields (Halliday et al. 2004; Milvang-Jensen et al. 2008). Spectroscopic targets were selected from I-band catalogues, producing an essentially I-band-selected sample with no selection bias down to $I = 22$ at $z \sim 0.4$–0.6 and $I = 23$ at $z \sim 0.6$–0.8 (Halliday et al. 2004; Milvang-Jensen et al. 2008). Typically, spectra of more than 100 galaxies per field were obtained.

HST/ACS mosaic imaging in $F814W$ of 10 of the highest-redshift clusters was also acquired (Desai et al. 2007), covering with four ACS pointings a 6.5×6.5-arcmin^2 field with an additional deep pointing in the centre. This field covers the R_{200} of all clusters, except for 1232.5−1250 where it reaches $0.5R_{200}$ (Poggianti et al. 2006). The R_{200} values for our structures are computed from the velocity dispersions by Poggianti et al. (2008).

2.2.1 *Morphologies, ellipticity measurements and galaxy stellar masses*

Morphologies are discussed in detail in Desai et al. (2007). The morphological classification of galaxies is based on the visual classification of *HST*/ACS $F814W$ images sampling the rest-frame ∼4500–5500 Å range, similarly to the WINGS.

The determination of ellipticities is presented in Simard et al. (2009). They have been estimated using the tool GIM2D version 3.2, a fitting program (Simard et al. 2002) that performs a detailed surface

Table 3. List of additional WINGS clusters used for the magnitude-'delimited' sample, their redshift, velocity dispersion, distance modulus (DM) and R_{200}.

Cluster name	z	σ (km s^{-1})	DM (mag)	R_{200} (kpc)
A85	0.0521	1052 ± 68	36.83	2.54
A133	0.0603	810 ± 78	37.16	1.95
A147	0.0447	666 ± 13	36.48	1.61
A160	0.0438	561 ± 53	36.44	1.36
A168	0.0448	503 ± 43	36.49	1.22
A193	0.0485	759 ± 59	36.67	1.83
A311	0.0657	NULL	37.35	0.00
A376	0.0476	852 ± 49	36.62	2.06
A548b	0.0441	848 ± 59	36.45	2.05
A602	0.0621	720 ± 73	37.22	1.73
A671	0.0507	906 ± 58	36.77	2.19
A780	0.0565	734 ± 10	37.01	1.26
A1291	0.0509	429 ± 49	36.77	1.04
A1668	0.0634	649 ± 57	37.27	1.56
A1736	0.0461	853 ± 60	36.55	2.06
A1795	0.0633	725 ± 53	37.27	1.74
A1831	0.0634	543 ± 58	37.27	1.30
A1983	0.0447	527 ± 38	36.48	1.28
A1991	0.0584	599 ± 57	37.08	1.44
A2107	0.0410	592 ± 62	36.29	1.44
A2124	0.0666	801 ± 64	37.38	1.92
A2149	0.0675	353 ± 53	37.41	0.85
A2169	0.0578	509 ± 40	37.06	1.22
A2256	0.0581	1273 ± 64	37.07	3.06
A2271	0.0584	504 ± 10	37.08	1.21
A2457	0.0584	580 ± 39	37.08	1.40
A2572a	0.0390	631 ± 10	36.18	1.53
A2589	0.0419	816 ± 88	36.34	1.98
A2593	0.0417	701 ± 60	36.33	1.70
A2622	0.0610	696 ± 55	37.18	1.67
A2626	0.0548	625 ± 62	36.94	1.51
A2657	0.0400	381 ± 83	36.23	0.92
A2665	0.0562	NULL	37.00	0.00
A2717	0.0498	553 ± 52	36.73	1.34
A2734	0.0624	555 ± 42	37.23	1.33
A3164	0.0611	NULL	37.19	0.00
A3497	0.0680	726 ± 47	37.43	1.74
A3528a	0.0535	899 ± 64	36.89	2.17
A3528b	0.0535	862 ± 64	36.89	2.08
A3530	0.0544	563 ± 52	36.92	1.36
A3532	0.0555	621 ± 53	36.97	1.50
A3558	0.0477	915 ± 50	36.63	2.21
A3667	0.0530	993 ± 84	36.87	2.39
A3716	0.0448	833 ± 39	36.49	2.07
A3880	0.0570	763 ± 65	37.03	1.84
A4059	0.0480	715 ± 59	36.64	1.73
IIZW108	0.0483	513 ± 75	36.66	1.24
MKW3s	0.0444	539 ± 37	36.47	1.30
RX0058	0.0484	637 ± 97	36.66	1.54
RX1022	0.0548	577 ± 49	36.94	1.39
RX1740	0.0441	582 ± 65	36.45	1.41
Z1261	0.0644	NULL	37.31	0.00
Z2844	0.0503	536 ± 53	36.75	1.29
Z8338	0.0494	712 ± 60	36.71	1.72
Z8852	0.0408	765 ± 63	36.28	1.86

brightness profile analysis of galaxies in low signal-to-noise ratio images in a fully automated way. In this paper, we use the ellipticities derived fitting every source in the *HST*/ACS images with a single Sérsic fit model. Since the shape of the PSF on the *HST*/ACS images varies significantly as a function of the position, spatially-varying PSF models for the EDisCS cluster images were constructed.

In this analysis, we consider only eight of the 10 EDisCS clusters for which *HST* images are available. In fact, ellipticity measurements are not available for 1227.9−1138 and no galaxies of 1037.9−1243 enter our final samples (see below the selection criteria).

For EDisCS galaxies, we use stellar masses estimated using the same relation we use for the WINGS data set, hence again following the Bell & de Jong (2001) method and then converting masses to a Kroupa (2001) IMF. Total absolute magnitudes are derived from photo-z fitting (Pelló et al. 2009) and rest-frame luminosities have been derived using Rudnick et al. (2003) and Rudnick et al. (2006) methods and presented in Rudnick et al. (2009). Stellar masses for spectroscopic members were also estimated using the KCORRECT tool (Blanton & Roweis 2007)[3] that yields masses in agreement with those used in this paper. For a detailed discussion of our mass estimates and of the consistency between different methods, see Vulcani et al. (2010a).

2.2.2 *Mass-limited sample*

For the EDisCS mass-limited sample, we use all photo-z members, following the membership criteria described above.

The choice to use the photo-z membership instead of spectroscopically confirmed members is dictated by the fact that, otherwise, the number of galaxies would be low, not allowing a statistically meaningful analysis.

Moreover, the spectroscopic magnitude limit ranges between $I = 22$ and 23 depending on redshift and the corresponding spectroscopic stellar mass limit is $M = 10^{10.6}\,\mathrm{M}_{\odot}$ (Vulcani et al. 2010b). The photo-z technique allows us to push the mass limit to much lower values than the spectroscopy. We adopt a conservative magnitude completeness limit for the EDisCS photometry equal to $I \sim 24$ (though the completeness remains very high to magnitudes significantly fainter than $I = 24$, White et al. 2005). We consider the most-distant cluster, 1216.8−1201, which is located at $z \sim 0.8$, and determine the value of the mass of a galaxy with an absolute B magnitude corresponding to $I = 24$ and a rest-frame colour $(B - V) \sim 0.9$, which is the reddest colour of galaxies in this cluster. In this way, the EDisCS mass completeness limit based on photo-z is $M_* = 10^{10.2}\,\mathrm{M}_{\odot}$. This is the mass limit we adopt for our analysis. As we discuss in Vulcani et al. (2010a), spectroscopic and photo-z techniques give very consistent results for the galaxy mass functions in the mass range in common. Also comparing the ellipticity distribution determined using spectroscopic and photo-z data down to the spectroscopic mass limit, we find that they are not statistically different: a Kolmogorov–Smirnov (K–S) test cannot reject the null hypothesis that the distributions are drawn from the same parent distribution with a probability of ∼22 per cent (for details on the K–S test, see Section 3). This gives additional support to our choice to use photo-z data.

As for the WINGS mass-limited sample, both BCGs and all galaxies at radii greater than $r = 0.6R_{200}$ have been excluded from the analysis. Table 4 presents the list of clusters used and some relevant values.

The final mass-limited EDisCS sample of galaxies with a measured ellipticity for $M_* \geq 10^{10.2}\,\mathrm{M}_{\odot}$ consists of 206 early-type

[3] http://cosmo.nyu.edu/mb144/kcorrect/

Table 4. List of EDisCS clusters analysed in this paper, with cluster name, redshift, velocity dispersion and R_{200} (from Halliday et al. 2004; Milvang-Jensen et al. 2008; Poggianti et al. 2008).

Cluster name	z	σ (km s^{-1})	R_{200} (Mpc)
1040.7−1155	0.70	418^{+55}_{-46}	0.70
1054.4−1146	0.70	589^{+78}_{-70}	0.99
1054.7−1245	0.75	504^{+113}_{-65}	0.82
1103.7−1245	0.62	336^{+36}_{-40}	0.41
1138.2−1133	0.48	732^{+72}_{-76}	1.41
1216.8−1201	0.79	1018^{+73}_{-77}	1.61
1232.5−1250	0.54	1080^{+119}_{-89}	1.99
1354.2−1230	0.76	648^{+105}_{-110}	1.08

galaxies, 145 of which are classified as ellipticals and 61 as S0s (see Table 2).

2.2.3 *Magnitude-'delimited' sample*

For the magnitude-'delimited' sample at high z, to follow the same criteria of Holden et al. (2009), we do not consider the photo-z membership, but we exclude only those galaxies that have been identified spectroscopically as non-members. Then, we use all early-type galaxies within 2σ of the red sequence and with $-19.3 > M_B + 1.208z > -21$.

To determine the red sequence of each cluster, as Mei et al. (2009) did, we use only spectroscopic members of our clusters (Halliday et al. 2004; Milvang-Jensen et al. 2008). We build colour–magnitude diagrams using the $R - I$ colour (that corresponds to $\sim B - V$ in the WINGS). Only for 1232.5−1250 we use the $V - I$ colour because the R band is not available.

Similarly to what we do for the WINGS, we determine the red sequence by performing a weighted least-squares fit of our data. However, since the resulting red sequences are not always reliable, for all clusters, but 1232.5−1250, for which we use a different colour, we determine a mean slope using only 1216.8−1201 and 1054.4−1146, two clusters located almost at the same redshift for which the red sequence is well defined from the spectroscopy, and adopt this slope for all clusters. The mean dispersion is determined by averaging the dispersion of all clusters except 1354.2−1230 that has been excluded, because, having too few points, it would give too small a value of the dispersion. Then, we determine separately the red sequence of each cluster, using the slope and the dispersion just determined and finding the most appropriate value of the intercept. Obviously, the red sequence for 1232.5−1250 is determined separately using its spectroscopic data.

Subsequently, we consider only galaxies within R_{200} (as for the WINGS), instead of $2R_{200}/\pi$ as Holden et al. (2009) did, to improve the statistics.

Our final sample consists of 101 ellipticals and 43 S0s, for a total of 144 early-type galaxies (see Table 2).

3 RESULTS: THE ELLIPTICITY EVOLUTION IN MASS-LIMITED SAMPLES

In this section, we analyse the ellipticities of galaxies in our mass-limited samples.

3.1 Ellipticity and S0/E number ratio as a function of the galaxy stellar mass

Fig. 5 shows the trend of the ellipticity as a function of the galaxy stellar mass for early-type, elliptical and S0 galaxies for the WINGS and EDisCS samples, above their mass completeness limits. We compute the median values of the ellipticity both over the whole mass range (green dashed lines) and in mass bins of 0.4 dex (red solid lines).

At both redshifts, the trend of the ellipticity of all early-type galaxies together clearly depends on the galaxy mass. Less-massive galaxies tend to have ellipticities that extend to much higher values compared to higher mass galaxies which populate only the lower end of the range. Considering only ellipticals, the trend is much less striking, though still present over the whole mass range in the WINGS, while a drop is observed only above $M_* \sim 10^{11.2}\,\mathrm{M}_\odot$ in the EDisCS. The median ellipticity of S0s shows no clear trend with the galaxy mass, at least below $M_* \sim 10^{11.1}\,\mathrm{M}_\odot$ in the WINGS. At high masses, both the apparent fall in the WINGS and the rise in the EDisCS may be simply due to low number statistics.

We note that ellipticals always have an ellipticity lower than 0.6 and mostly below 0.4, while S0s cover a wider range of ellipticities, with the majority being concentrated at high values of ellipticities, above 0.4. Furthermore, ellipticals reach higher mass values than S0s (see Vulcani et al. 2010a for the mass distribution of ellipticals and S0s in these samples, see also Section 5).

Clearly, the strong trend of the ellipticity with mass observed in early types is due both to the trend of the ellipticity of elliptical galaxies with mass and, mostly, to the fact that the ellipticals and S0s are found in different proportions at different masses: S0 galaxies, with their average higher ellipticities, become more frequent going to lower masses. Fig. 6 shows the ratio of the number of S0 to elliptical galaxies at different masses. In the WINGS (left-hand panel), the S0-to-elliptical ratio strongly depends on mass: at higher masses, there are proportionally more elliptical galaxies than at lower masses. In the highest-mass bin, the ratio drops to $\sim$0, indicating that there are almost only elliptical galaxies, while at $M_* \sim 10^{10.5}\,\mathrm{M}_\odot$ S0s are twice as numerous as ellipticals. In contrast, in the EDisCS (right-hand panel), we find that the trend is almost flat up to $M_* \sim 10^{11.5}\,\mathrm{M}_\odot$ and S0s are less than half of the ellipticals.

EDisCS clusters are seen at an epoch prior to the build-up of the S0 cluster population and Fig. 6 clearly shows that such build-up occurs mainly at masses below $10^{11}\,\mathrm{M}_\odot$.

3.2 The evolution of the median ellipticity and of the ellipticity distributions

Table 5 summarizes the median values of ellipticities for both samples over the whole range of masses. Errors are estimated using the bootstrap resampling method. We adopt these estimates because we want to characterize the errors on the medians and not the dispersion of the points around the median value (that is the standard deviation). In the WINGS, the choice of the mass limit ($M_* \geq 10^{9.8}\,\mathrm{M}_\odot$ or $M_* \geq 10^{10.2}\,\mathrm{M}_\odot$) does not alter the final results.

Comparing low- and high-z, the median ellipticity of S0s is compatible within the errors at the two redshifts, while it slightly changes with redshift for ellipticals and more notably for early types. In particular, it slightly *decreases* going to the current epoch for ellipticals, while it clearly *increases* for the early types. This raise for early types is due to the fact that, as shown in Fig. 6, the fraction of S0s increases at low z, mainly in the low mass range. Since S0s are more flattened than ellipticals, the median ellipticity of early types shifts

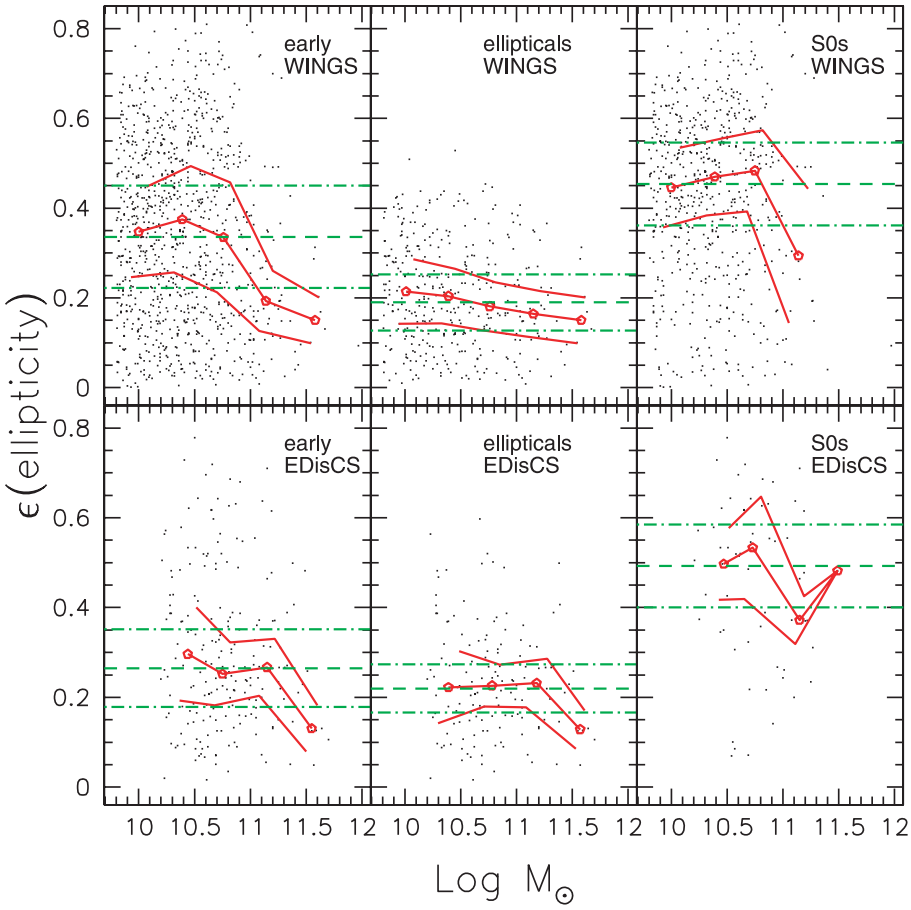

Figure 5. Ellipticity versus mass in the mass-limited sample. Black points: galaxies. Red solid lines: median and 1σ values, where σ is the rms, estimated in mass bins. Green dashed lines: median and 1σ values computed over the whole mass range. Top panels: WINGS data (left-hand panel: early-type galaxies; middle panel: elliptical galaxies; and right-hand panel: S0 galaxies). The WINGS medians are corrected for spectroscopic incompleteness. Bottom panels: EDisCS data (rest of the description is the same as for the WINGS).

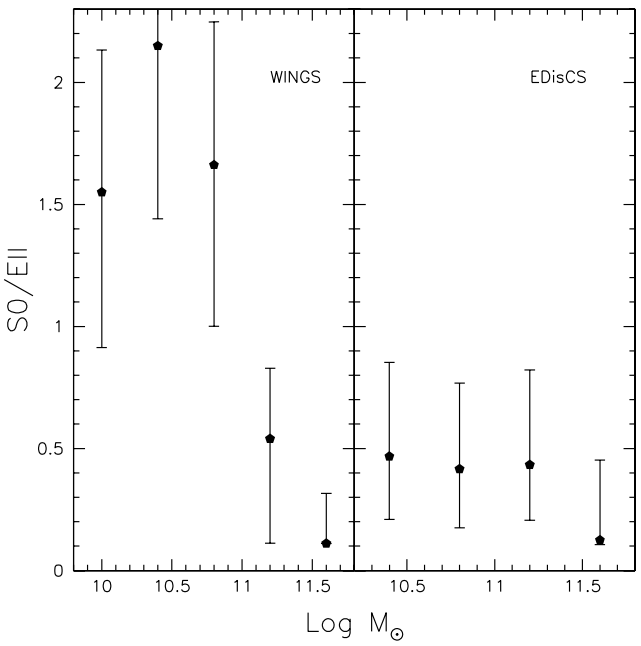

Figure 6. Ratio of the number of S0 to elliptical galaxies at different masses both for the WINGS (left-hand panel) and for the EDisCS (right-hand panel) in our mass-limited sample. Errors are binomial (Gehrels 1986).

Table 5. Ellipticity median values for both mass-limited samples with errors defined with bootstrap resampling. For the WINGS, medians are computed taking into account the weights. For the WINGS, values above the EDisCS mass limit are also given.

	WINGS		EDisCS
	$M_*/\mathrm{M}_\odot \geq 10^{9.8}$	$M_*/\mathrm{M}_\odot \geq 10^{10.2}$	$M_*/\mathrm{M}_\odot \geq 10^{10.2}$
Ellipticals	0.190 ± 0.011	0.179 ± 0.011	0.220 ± 0.011
S0s	0.454 ± 0.014	0.462 ± 0.015	0.493 ± 0.032
Early types	0.336 ± 0.012	0.328 ± 0.016	0.265 ± 0.013

to higher values at low redshift. As for the evolution of the median of elliptical galaxies, this will be discussed later in this section.

We now compare the high- and low-z ellipticity distribution to see if it evolves. At both redshifts, we consider only galaxies above the common mass limit, that is, $M_* = 10^{10.2}\,\mathrm{M}_\odot$.

We build both the cumulative distributions and histograms (in bins of ellipticity equal to 0.05) for each class of galaxies analysed. For the WINGS, both of them take into account the spectroscopic completeness weights.

Fig. 7 shows how the ellipticity distribution of early-type galaxies evolves with redshift. As expected, given the evolution of the median ellipticity, there are proportionally more galaxies with higher ellipticities at low- than at high-z, indicating that low-z early-type

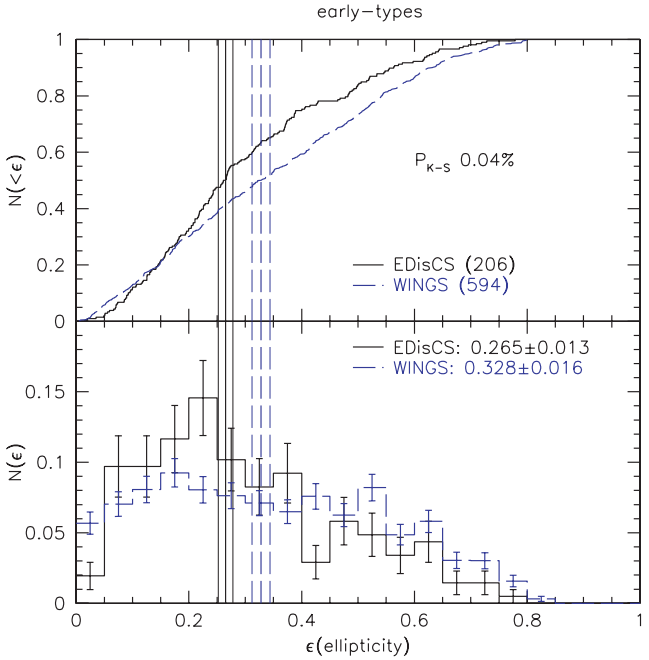

Figure 7. Comparison of ellipticity distributions of early-type galaxies in the mass-limited samples. Medians and bootstrap errors are also indicated. Black solid lines: EDisCS; blue dashed lines: WINGS. Top panel: cumulative distributions of ellipticity. P_{K-S} is the probability that the two distributions are drawn from the same parent distribution. The numbers in brackets are the number of galaxies in the considered samples. Bottom panel: histograms in bins of 0.05 dex, normalized to 1.

galaxies are on average more flattened. The overall WINGS distribution (blue dashed lines) is quite flat, in particular, at intermediate values of ellipticity. Instead, the ellipticity distribution of EDisCS early-type galaxies (black solid lines) shows a peak around $\epsilon \sim 0.2$.

To quantify the differences between the two distributions, we perform a K–S test.[4] Throughout this paper, we will consider two significantly different distributions if the K–S test gives a probability <5 per cent. For early-type galaxies, the K–S test allows us to exclude the similarity of the ellipticity distributions at the two redshifts, giving a probability of ∼0.04 per cent.

Next, we investigate whether the observed differences are due to an evolution of the ellipticity distribution of ellipticals, of S0s or both. Fig. 8 shows that for ellipticals results are ambiguous: the K–S test, giving a probability of 5.84 per cent of similarity of the distributions, is not strictly conclusive. In contrast, for S0s, the distributions are compatible with being similar ($P_{K-S} \geq 20$ per cent). EDisCS S0s are very few and this could influence the results of the K–S test; however, the cumulative distributions appear to resemble each other, indicating that the result of the K–S test should be reliable.

We wish to go deeper into our analysis, trying to understand if the K–S results are confirmed and above all if they are driven by a different shape of the distributions or simply by a different location of the two populations. To do this, we perform two other statistical non-parametric tests (i.e. they do not assume the normal distribution) which make no assumptions about the distributions of the populations.

In Appendix A, we present the detailed analysis of the Moses (1963) and Mann & Whitney (1947) tests. In summary, although the K–S test is inconclusive, from these additional tests, it emerges that some mild differences exist in the ellipticity distribution of ellipticals at high- and low-z.

3.2.1 *Round ellipticals at low z*

Inspecting the histograms in Fig. 8, it is clear that, at both redshifts, there are no ellipticals with $\epsilon \geq 0.6$ and both distributions are peaked around $\epsilon \sim 0.2$–0.3. It seems that the greatest differences are confined to the extremes of the distributions: in the highest ellipticity bins, there are proportionally more EDisCS elliptical galaxies than WINGS' and more notably, in the first bin, there are proportionally more WINGS galaxies with $\epsilon \leq 0.05$ than EDisCS galaxies. It is important to stress that this goes in the opposite direction of what could be expected from morphological classification biases at high z: face-on S0s would be systematically mistaken for ellipticals more frequently at high- than at low-z. Analysing more accurately the first bin (plot not shown), we find that it is mainly dominated by a second peak around $\epsilon \sim 0.03$ that instead is not detected in the EDisCS distribution. At the moment, we are not able to explain why at low z there is an exceeding population of rounder ellipticals compared to high z; anyway, we think it is real, having accurately checked both morphologies and ellipticities for those galaxies.[5]

We have also visually inspected the ellipticity profiles of these round WINGS ellipticals. For a few of them, the profile is altered by crowding, while for some others, the twist of the isophotes is very marked and the ellipticity value strongly changes with the radius. However, 60 per cent of the analysed galaxies really have a very low ellipticity at all radii. Analysing and understanding this population goes beyond the scope of this work and it will be discussed in a forthcoming paper. Here, we just note that this population exists and that it could be the result of dry merger events (van Dokkum et al. 1999; Tran et al. 2005) which might preferentially result in round galaxies building over time.

If elliptical galaxies with $\epsilon < 0.05$ are excluded, the WINGS and EDisCS ellipticity distributions for ellipticals are indistinguishable (the K–S test gives a probability >20 per cent that the populations are drawn from the same parent distribution).

3.3 What drives the evolution of the ellipticity distribution of early-type galaxies: the evolution of the galaxy mass distributions or the evolution of the relative proportions of ellipticals and S0s?

To summarize the most-important points, in the previous sections, we have found that, for mass-limited samples, the ellipticity distribution of early-type galaxies strongly changes with redshift. The ellipticity distributions of ellipticals and S0s on the whole do not evolve significantly, although for ellipticals there is a non-negligible

[4] The standard K–S test, in building the cumulative distribution, assigns to each object a weight equal to 1. Instead, our WINGS data are characterized by spectroscopic completeness weights. So, we modified the test to make the relative importance of each galaxy in the cumulative distribution depend on its weight and not being fixed to 1. In the following, we will always use this modified K–S test. Obviously, when using photo-z, all galaxies have a weight equal to 1 and using the modified test is equivalent to using the standard one.

[5] We find a similar peak also in our low-z magnitude-'delimited' sample (see Section 4) and in the low-z sample analysed by Holden et al. (2009) (see Section 6), so it can be neither due to the adopted selection criteria nor due to a bias in our samples.

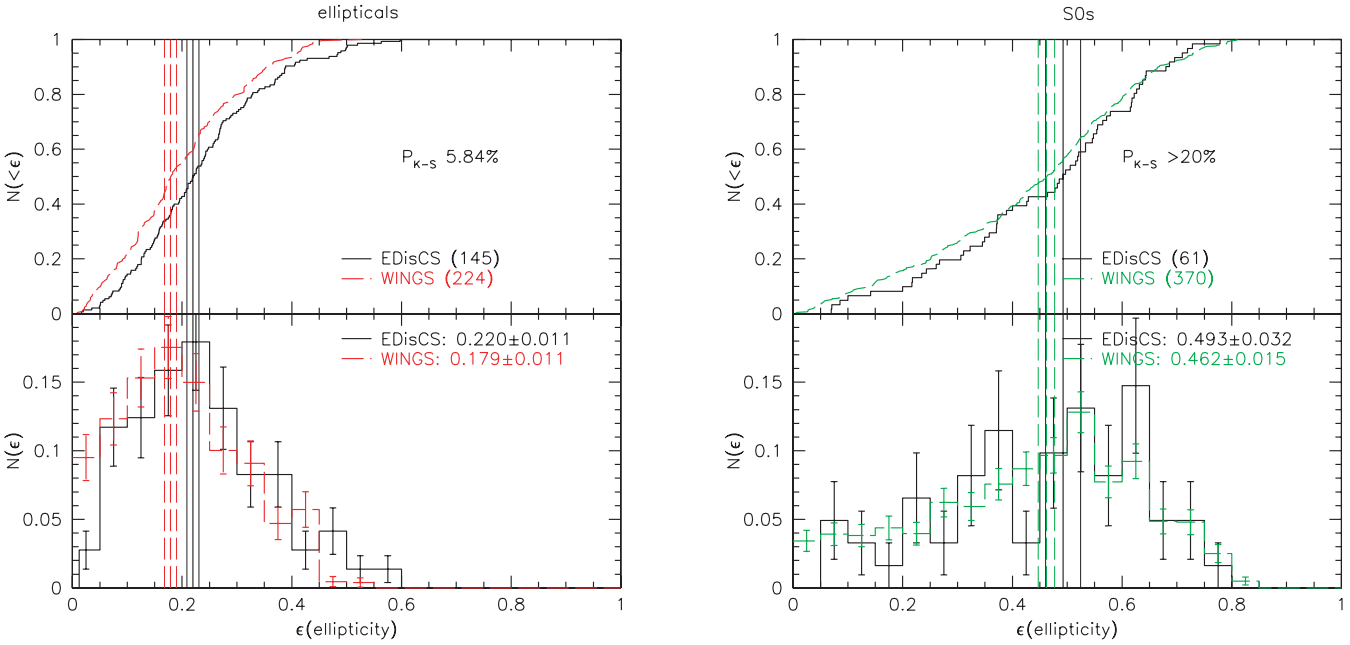

Figure 8. Comparison of ellipticity distributions of elliptical (left-hand panel) and S0 (right-hand panel) galaxies in the mass-limited samples. The medians and their bootstrap errors are also indicated. Black solid lines: EDisCS; red (left-hand panel) and green (right-hand panel) dashed lines: WINGS. Top panels: cumulative distributions of ellipticity. P_{K-S} is the probability that the two distributions are drawn from the same parent distribution. The numbers in brackets are the number of galaxies in the considered samples. Bottom panels: histograms in bins of 0.05 dex, normalized to 1.

shift in the medians of the distributions due to a relative excess of round ellipticals at low z compared to high z.

We have found in Fig. 5 that above all for early types there is a trend of ellipticity with mass and that these trends are different in the EDisCS and WINGS. Moreover, as we have discussed at length in a previous paper (Vulcani et al. 2010a), the WINGS and EDisCS have different galaxy stellar mass distributions. We have found that the mass distribution of *each* morphological type evolves with redshift and that all types have proportionally more massive galaxies at high$z$ than at low z. As a consequence, if we want to understand the origin of the ellipticity distribution of galaxies of different morphological types and at different redshifts, we have to try to disentangle the influence of the evolution of the mass distribution from the effects of the morphological evolution.

3.3.1 The evolution of the galaxy mass distribution

First, we analyse separately ellipticals and S0s. We perform 1000 Monte Carlo simulations extracting randomly from the WINGS sample a subsample with the same mass distribution as the EDisCS sample, separately for the two different morphological classes. Each time we extract from the WINGS the same number of galaxies that are in the EDisCS sample (i.e. 145 ellipticals and 61 S0s). For each simulation, we determine the ellipticity distribution, the median value of the ellipticity and we perform a K–S test to compare the result of the simulation with the EDisCS data set. Then, taking into account all the simulations, we determine both the median value of the K–S test and the fraction of simulations that give a conclusive statement (see Table 6).

Fig. 9 shows our results for the two morphological classes. The plotted WINGS histogram and cumulative distribution (dashed lines) are the average of the 1000 Monte Carlo simulations. The K–S probabilities and WINGS medians reported in the plots are the medians of the values of all the simulations. Adopting the same mass distribution, for elliptical galaxies, the match of the mass distributions at high z and low z makes the ellipticity distribution of WINGS galaxies (red dashed lines in the left-hand panel of Fig. 9) become significantly different from the EDisCS one. The K–S test gives conclusive results ($P_{K-S} \leq 5$ per cent) in 80 per cent of the simulations, with a median value of 1.3 per cent, rejecting the null hypothesis of similarity of the two distributions. This seems to imply that WINGS ellipticals tend to be on average rounder than EDisCS ellipticals of the same mass. This effect is mitigated in the observed WINGS versus EDisCS distributions (Fig. 8) (yielding a non-significant K–S test) by the fact that (i) there are proportionally more less massive galaxies at low z than at high z (for details on the mass functions, see Vulcani et al. 2010a); and (ii) low-mass ellipticals are more flattened (on average) than high-mass ones. Hence, the increase in the number of low-mass ellipticals at low z largely compensates the existence of a significant evolution in the ellipticity distribution of ellipticals with the same mass distribution (Fig. 9) and produces an ambiguous or at best weak evidence for evolution in our analysis of Section 3.2.

If we neglect galaxies with $\epsilon < 0.05$,[6] for which the most-outstanding differences are detected (see Section 3.2), adopting the same mass distribution, the median value of the K–S test is ∼8 per cent, indicating that the major difference between the ellipticals at high z and low z is indeed the enhanced population of round ellipticals at low z. Turning to S0s (green dashed lines in the right-hand panel of Fig. 9), the mass-matched ellipticity distributions of the WINGS and EDisCS remain statistically indistinguishable: the K–S test cannot reject the null hypothesis, giving a probability

[6] In this way, we wish to compare the whole general distribution without being too much influenced by galaxies located in only one bin.

Table 6. Results of the K–S test performed on the 1000 mass-matched and morphology-matched simulations (see Section 3.3). P_{K-S} is the probability that the WINGS and EDisCS distributions are drawn from the same parent distribution.

	P_{K-S}				
	<1 per cent	1–5 per cent	5–10 per cent	>10 per cent	Median
			Mass-matched simulations		
Ellipticals	50 per cent	30 per cent	9 per cent	11 per cent	1.3 per cent
S0s	1 per cent	6 per cent	4 per cent	89 per cent	>20 per cent
Early types	18 per cent	30 per cent	20 per cent	32 per cent	5.2 per cent
			Morphology-matched simulations		
Early types	0 per cent	3 per cent	8 per cent	89 per cent	>20 per cent

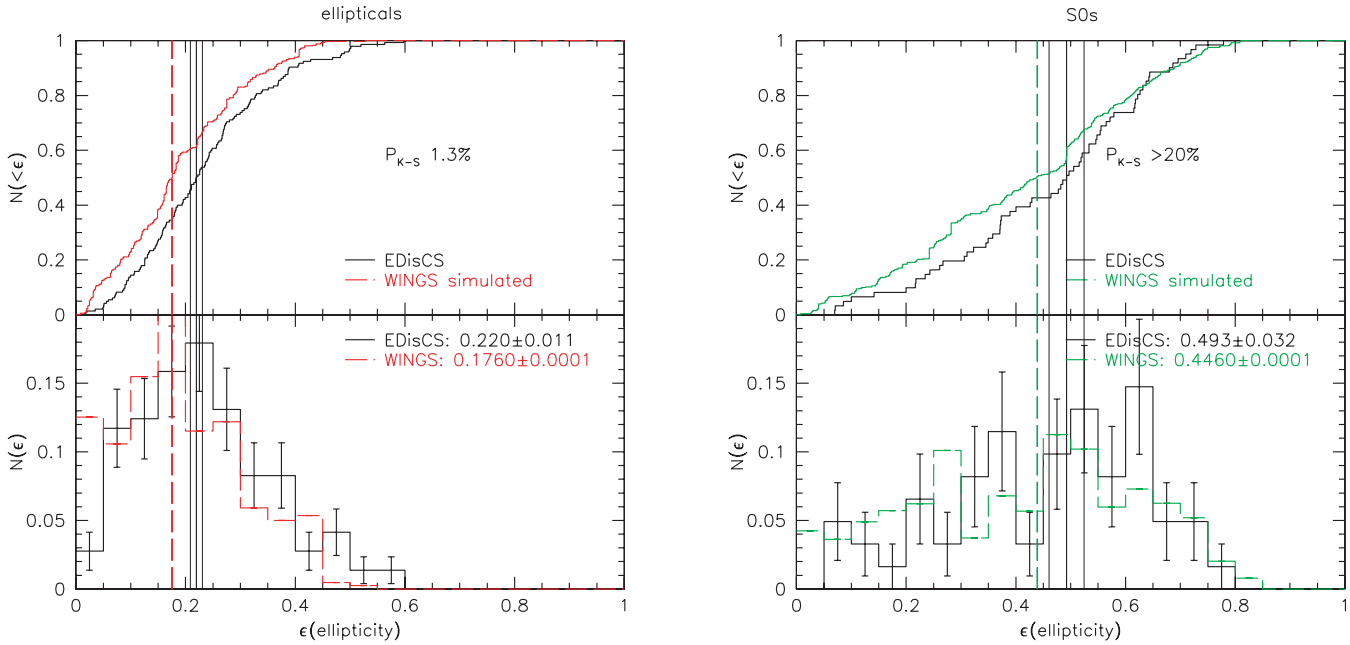

Figure 9. Ellipticity distribution of elliptical (left-hand panel) and S0 (right-hand panel) galaxies, assuming the same mass distribution for the WINGS as for the EDisCS (cf. Fig. 8). Panels and symbols are the same as in Fig. 8. The plotted WINGS histogram and cumulative distributions are the average of the 1000 Monte Carlo simulations. The P_{K-S} is the median K–S value.

≥5 per cent in 93 per cent of the simulations and a median value >20 per cent.

Now we wish to test if the different mass distribution at different redshifts alters the ellipticity distribution of early types, so we put together WINGS ellipticals and S0s, being sure to extract randomly galaxies in order to have the same EDisCS mass distribution and maintaining the WINGS morphological fractions (i.e. ∼40 per cent ellipticals and ∼60 per cent S0s – see Table 7). In this way, we test whether the observed evolution of the ellipticity distribution of early-type galaxies can be entirely explained by the evolution of the mass distributions.

In Fig. 10, the K–S test gives a probability ≤5 per cent that the two distributions are driven from the same parent distribution in 48 per cent of the simulations (Table 6) and a median probability for all simulations of 5.2 per cent. Excluding galaxies with $\epsilon < 0.05$, the K–S test results remain similar (median $P_{K-S} \sim 4$ per cent, $P_{K-S} < 5$ per cent in 55 per cent of the simulations, plot not shown). These values suggest that the different mass distribution at

Table 7. Relative morphological fractions of galaxies in both mass and magnitude-(de)limited samples. For the WINGS mass-limited sample, numbers above the EDisCS mass limit are also given. In both cases, both observed and completeness-weighted numbers are listed. Errors are binomial, as defined in Gehrels (1986).

	WINGS					EDisCS	
	Mass limited				Magnitude (de)limited	Mass limited	Magnitude (de)limited
	$M_* \geq 10^{9.8}\,M_\odot$		$M_* \geq 10^{10.2}\,M_\odot$			$M_* \geq 10^{10.2}\,M_\odot$	
	Per cent$_{obs}$	Per cent$_w$	Per cent$_{obs}$	Per cent$_w$	Per cent	Per cent	Per cent
Ellipticals	38.3 ± 1.7	37.9 ± 1.3	37.7 ± 2.1	37.1 ± 1.7	38.8 ± 1.3	70.4 ± 3.3	70.1 ± 4.0
S0s	61.7 ± 1.7	62.1 ± 1.3	62.3 ± 2.1	62.9 ± 1.7	61.2 ± 1.3	29.6 ± 3.3	29.9 ± 4.0

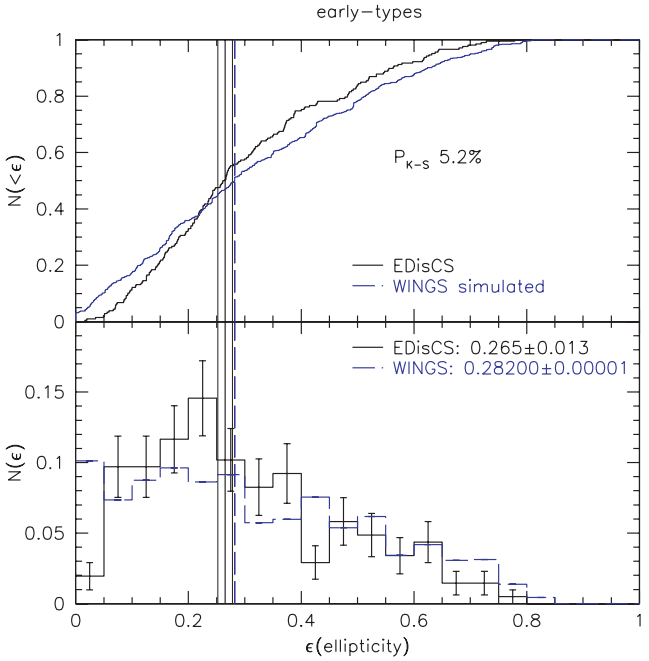

Figure 10. Ellipticity distribution of early-type galaxies assuming for the WINGS the same mass distribution as for the EDisCS galaxies and maintaining the WINGS morphological mix (cf. Fig. 7). Panels and symbols are the same as in Fig. 7. The plotted WINGS histogram and cumulative distributions are the average of the 1000 Monte Carlo simulations. The P_{K-S} is the median K–S value.

the different redshifts influences at some level the evolution of the ellipticity distribution, even if probably it is not the main factor as it cannot fully explain the observed evolution.

3.3.2 The evolution of the morphological fractions

We now wish to assess the role played by the evolution with redshift of the relative morphological fractions. In Table 7, we show how much the morphological fractions change with time, both for the mass-limited sample and for the magnitude-'delimited' one (see Section 4). We observe that while at high redshift ellipticals are more common than S0s (∼70 per cent and ∼30 per cent, respectively), in the local Universe S0s dominate, representing ∼62 per cent of the early types.

To analyse the importance of this evolution, we now perform a second test, extracting randomly from the WINGS data set a subsample of galaxies with approximately the same relative fraction of S0s and ellipticals as the EDisCS (i.e. in each simulation we extract 70 ellipticals and 30 S0s from the WINGS sample) and paying attention to maintain the WINGS mass distribution. In this way, we wish to test whether the morphological evolution can account for the ellipticity evolution of early-type galaxies, letting the mass distribution to naturally evolve. We perform 1000 such simulations.

We then compare the ellipticity distribution of the 'modified' WINGS sample to the real EDisCS one. Considering all galaxies (also those with $\epsilon < 0.05$) (plot not shown), the K–S test is conclusive ($P_{K-S} \leq 5$ per cent) in 69 per cent of the simulations, while the median value of the probability is 0.2 per cent, indicating that even assuming the same morphological fraction in the two samples, differences between the two ellipticity distributions are still detected.

Next, we exclude from our analysis those galaxies (both ellipticals and S0s) with $\epsilon < 0.05$, since their presence likely alters the final results. In fact, increasing the number of elliptical galaxies in the WINGS from being ∼40 to ∼70 per cent of the whole population, the contribution of galaxies with $\epsilon \sim 0.03$ is hugely magnified and it would strongly influence the whole population. For galaxies with $\epsilon \geq 0.05$, Fig. 11 shows that, if at both redshifts we had the same fractions of ellipticals and S0s, the ellipticity distributions for early-type galaxies would be indistinguishable. The K–S test is conclusive ($P_{K-S} \leq 5$ per cent) only in 3 per cent of the simulations, while the median value of the probability is >20 per cent.

Importantly, doing the same in the observed distributions and excluding all galaxies with $\epsilon < 0.05$ from Fig. 7, the low- and high-z early-type ellipticity distributions remain significantly different, with a K–S test probability to be drawn from the same parent distribution of only 0.002 per cent. Except for the excess of round ellipticals at low z, the evolution of the ellipticity distribution of early-type galaxies can be fully explained by the morphological evolution.

From this whole section, we conclude that it is mainly the relative contribution of each morphological type to the total that is responsible for the evolution of the ellipticity distribution of early-type galaxies, even if the role of the evolution of the mass distribution with redshift is non-negligible. The morphology appears to be the most-decisive factor in the evolution of the ellipticity distribution of early-type galaxies: the WINGS and EDisCS have a different morphological mix and their ellipticity distribution is regulated by the different relative proportions of ellipticals and S0s.

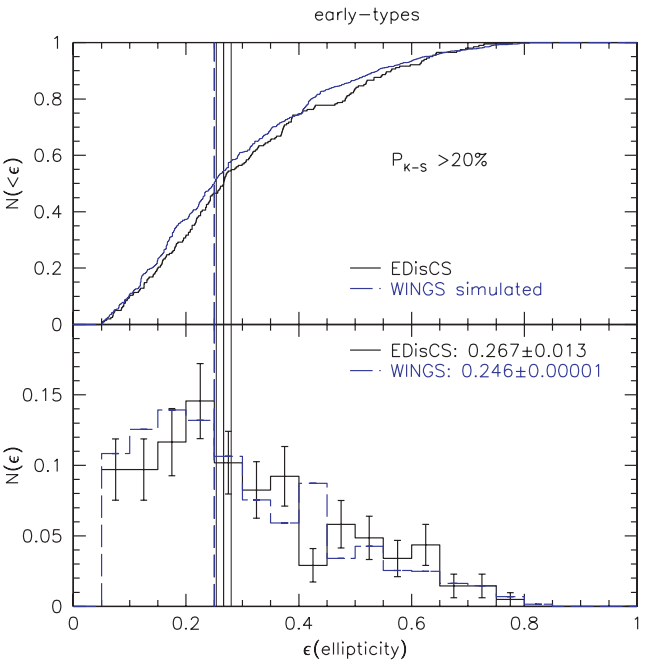

Figure 11. Ellipticity distribution of EDisCS and WINGS early-type galaxies, assuming for the WINGS the same fraction of ellipticals and S0s as for the EDisCS and maintaining the WINGS mass distribution (compare betweenFigs 7 and 10). Panels and symbols are the same as in Fig. 7. Only galaxies with $\epsilon \geq 0.05$ are considered.

Table 8. Ellipticity median values for the magnitude-'delimited' samples with errors estimated with bootstrap resampling. Holden et al. (2009) is the sample we use for comparison with the magnitude-'delimited' sample (for details, see Section 5).

	WINGS Magnitude delimited	EDisCS Magnitude delimited	Holden et al. (2009) Low z	Holden et al. (2009) High z
Ellipticals	0.176 ± 0.0073	0.218 ± 0.01	0.18 ± 0.010	0.20 ± 0.010
S0s	0.440 ± 0.0088	0.519 ± 0.034	0.38 ± 0.020	0.47 ± 0.020
Early types	0.300 ± 0.0093	0.265 ± 0.021	0.29 ± 0.020	0.30 ± 0.010

4 RESULTS: THE ELLIPTICITY DISTRIBUTION IN THE MAGNITUDE-'DELIMITED' SAMPLE

From the EDisCS and WINGS, we have also selected a magnitude-'delimited' sample of galaxies following the criteria adopted by Holden et al. (2009), as described in Section 2, with the aim to directly compare our finding with their results.

First of all, we wish to check if the different selection criteria implicate a change in our findings compared to the mass-limited sample.

In the magnitude-'delimited' sample, we qualitatively find the same ellipticity–mass relation we found in Fig. 5 (plots not shown) for the mass-limited sample: no trend of the ellipticity with the mass for S0s, slight trend for ellipticals and a striking trend for early-type galaxies.

Values of the median ellipticities of the different morphological types can be found in Table 8.

Analysing the ellipticity distributions in the magnitude-'delimited' sample, for early-types (Fig. 12) the K–S test cannot detect a significant evolution with redshift, as it gives a probability of ∼7.7 per cent that the two populations are drawn from the same parent distribution. However, the median ellipticities are different: the median is *higher* at low z (see also Table 8).

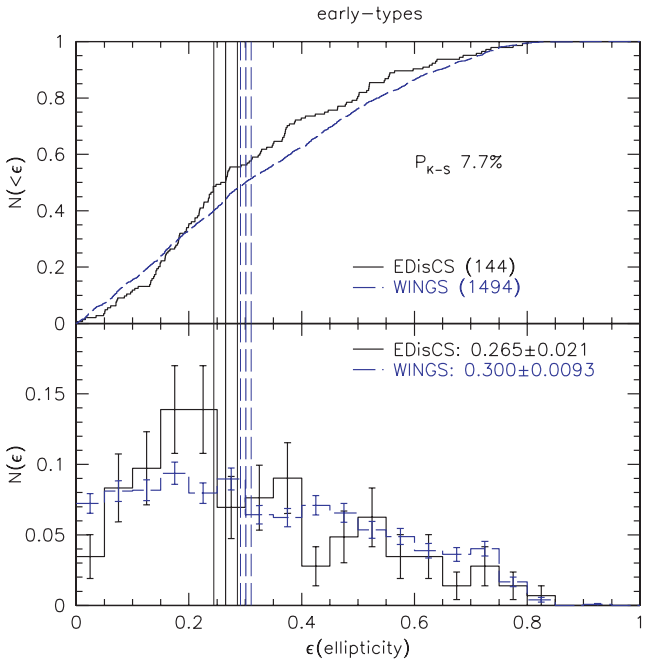

Figure 12. Ellipticity distribution of early-type galaxies in the magnitude-'delimited' samples. Panels and symbols are the same as in Fig. 7 (compare with the mass-limited sample shown in Fig. 7).

Fig. 13 shows separately the ellipticity distribution for elliptical and S0 galaxies. We find that the ellipticity of elliptical galaxies evolves notably with redshift: in the WINGS (red dashed lines in the left-hand panel of Fig. 13), there are proportionally more galaxies with low values of ellipticity, ($\epsilon < 0.15$), while in the EDisCS (black solid lines), there is a notable peak around $\epsilon \sim 0.2$. The K–S test excludes that elliptical galaxies have a common ellipticity distribution at different redshifts, giving a probability of ∼0.41 per cent that they are drawn from the same parent distribution. In contrast, the same test cannot distinguish any differences between the distributions of S0s, giving a probability of ∼12 per cent. However, we note that the median ellipticity of S0s is significantly *lower* at low z.[7]

4.1 How can results from different samples be reconciled?

Our mass- and magnitude-(de)limited samples give different results. In Appendix B, we discuss the reasons for the observed discrepancies, comparing directly the ellipticity distributions of the mass-limited and magnitude-'delimited' samples for the same type of galaxies at the same redshift. Briefly, the origin of the observed differences in the distributions lies in the fact that galaxies in the two samples are characterized by different properties; in particular, the magnitude-'delimited' samples are biased and so they are not representative of the overall population. In fact, selecting early-type galaxies on the red sequence only in the magnitude range $-19.3 > M_B + 1.208z > -21$, we are loosing (the few) most-massive galaxies and a large fraction of the less-massive galaxies.

5 COMPARISON WITH LITERATURE RESULTS

We now show that, even adopting the same selection criteria, our results are not in agreement with those reached by Holden et al. (2009) who investigated the evolution in the ellipticity distribution using two magnitude-'delimited' samples of cluster early-type galaxies in two redshift ranges. Their sample in the local Universe ($z = 0.02$–0.05) consisted of 10 clusters (for a total of 210 galaxies), while the sample in the distant Universe ($z = 0.33$–1.26) consisted of 17 clusters (for a total of 487 galaxies) of galaxies with *HST* images.

With this selection, their main conclusion is that there is no evolution neither in the median ellipticity nor in the shape of the ellipticity

[7] Performing the Moses test, we can conclude that the early types are unlikely to have the same scale parameter (with a probability of <5 per cent in 53 per cent of the simulations), while for both ellipticals and S0s, we cannot exclude a compatibility of the scale parameter, with a probability <5 per cent in 39 and 10 per cent of the simulations, respectively. From the Mann–Whitney test, we cannot exclude compatible medians for early types (with a probability of ∼14 per cent), while we can do it for ellipticals and S0s (with a probability of 0.07 and 3.4 per cent, respectively) (for details on the tests see Appendix A).

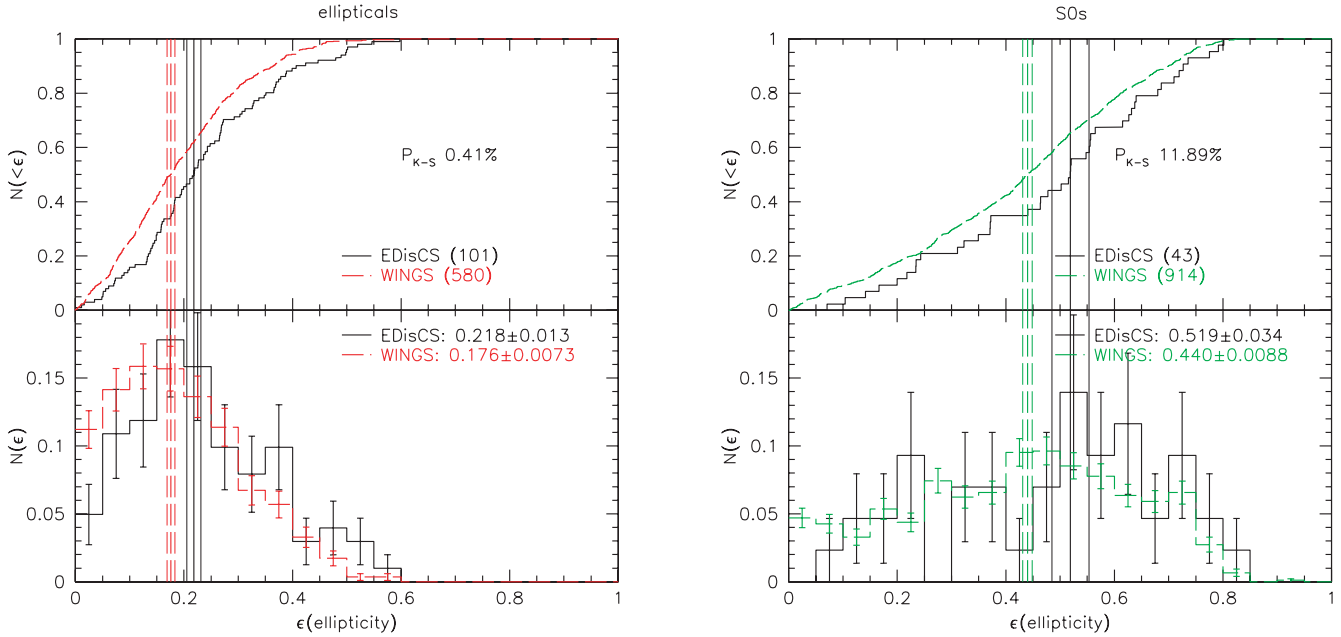

Figure 13. Ellipticity distribution of elliptical and S0 galaxies in our magnitude-'delimited' samples. Panels and symbols are the same as in Fig. 8 (compare with the mass-limited sample shown in Fig. 8).

distribution of cluster early-type galaxies with redshift from $z > 1$ to $z \sim 0$. Their median ellipticity at $z > 0.3$ is statistically identical to that at $z < 0.05$ and the shapes of the distributions broadly agree. Moreover, they find a statistically significant evolution in the S0 ellipticity distribution, while they do not detect evolution for the ellipticals.

In Table 8, we compare our median ellipticities with theirs.

Summarizing, comparing the two magnitude-'delimited' samples selected in the same way, even if we both do not detect an overall evolution in the ellipticity distribution for early-types galaxies, we do find an evolution in the median which they do not. Moreover, we find a significant evolution for ellipticals and no evolution for S0s (though again we do find an evolution in the median), while they find no evolution for ellipticals and strong evolution for S0s. This led us to believe that the agreement for the early types is not real, but simply due to a particular combination of the distributions of ellipticals and S0s.

We note that both at low z and at high z, there are some clusters that are in common between our and their samples: at low z, there are four: A119, A168, A957x and A1983; at high z, there are five: 1040.7−1155, 1054.4−1146, 1054.7−1245, 1216.8−1201 and 1232.5−1250. For these five EDisCS clusters in common at high z, also the morphological classifications (Desai et al. 2007) and the images used to measure ellipticities are the same.

So we can use this information to try to understand the reason for the discrepancy of the results.

5.1 Origin of the discrepancies

We proceed by comparing separately our WINGS and EDisCS samples with the Holden et al. (2009) samples, trying to identify the reason of the observed differences.

5.1.1 WINGS and Holden et al. (2009)

In Fig. 14, we compare our results at $0.04 < z < 0.07$ with those of Holden et al. (2009) at $z < 0.05$. While the ellipticity distributions of early-type galaxies and ellipticals are consistent with being similar in the two samples (in both cases the K–S test cannot reject the null hypothesis of similarity of the distributions, giving a probability of >20 per cent[8]), those of S0s are remarkably different: WINGS S0s (black solid lines in the right-hand panel of Fig. 14) peak around $\epsilon \sim 0.5$, while S0s of Holden et al. (2009) (green dashed lines in the same plot) peak around $\epsilon \sim 0.3$–0.35, indicating that in the Holden et al. (2009) sample galaxies are on average rounder than in the WINGS. The K–S test finds that the distributions can be drawn from the same parent distribution with a probability of only ∼2.3 per cent.

Since we adopted Holden et al. (2009) selection criteria, if there are differences, they can be due to either differences in the morphological classification or differences in the measurement of the ellipticities or variations in some other galaxy properties. Here we try to analyse each one of these factors.

Since Holden et al. (2009) draw morphologies from Dressler (1980) and in their sample at low z there are some clusters in common with the WINGS, we select from the catalogue of Dressler (1980) galaxies in common with the WINGS and see if there are some notable differences among them. On the whole, there are 18 clusters in the Dressler (1980) catalogue that also belong to the WINGS[9].

First of all, we select those galaxies that are early types according to the Dressler (1980) classification and we assign to them our measurements of ellipticity. In this way, we can compare directly our values of ellipticity with those calculated by Holden et al. (2009). Fig. 15 shows the ellipticity distribution of the two data sets, for early-type, elliptical and S0 galaxies: the K–S probability is always inconclusive ($P_{\rm K-S} \geq 20$, ∼8.5 and ≥20 per cent, respectively).

[8] This could be a problem linked to the poor statistic: if we double the number of Holden et al. (2009) galaxies, then the test becomes conclusive.
[9] For this comparison, we include in the analysis also those clusters from Dressler (1980) that do not enter the Holden et al. (2009) sample, in order to improve the statistics.

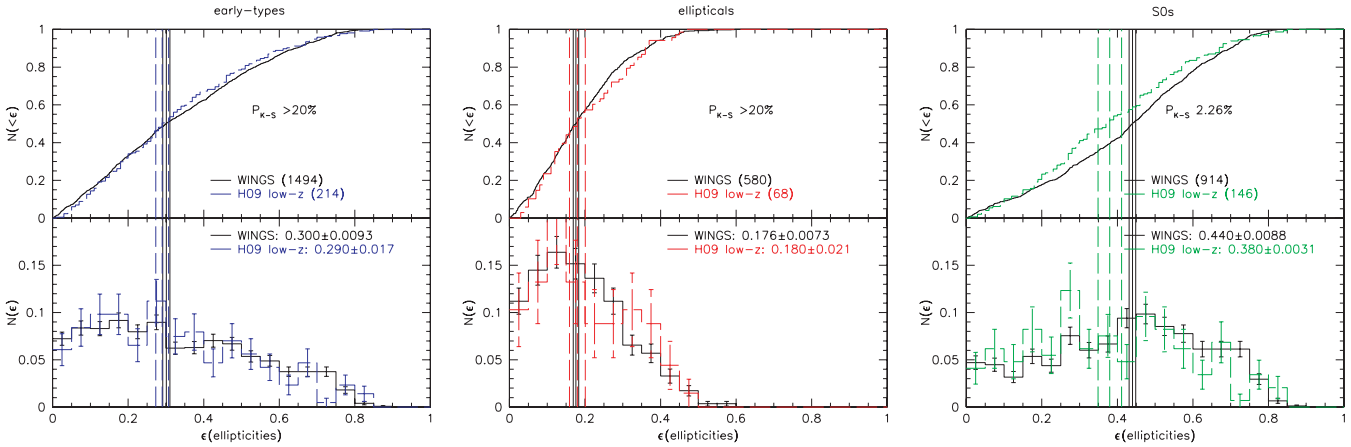

Figure 14. Comparison between our results and those of Holden et al. (2009) at low z. Top panels: cumulative distributions; bottom panels: histograms normalized to 1. P_{K-S} is the probability of the two distributions drawn from the same parent distribution. Left-hand panel: comparison between WINGS (black solid lines) and Holden et al. (2009) (blue dashed lines) early types. Middle panel: comparison between WINGS (black solid lines) and Holden et al. (2009) (red dashed lines) ellipticals. Right-hand panel: comparison between WINGS (black solid lines) and Holden et al. (2009) (green dashed lines) S0s.

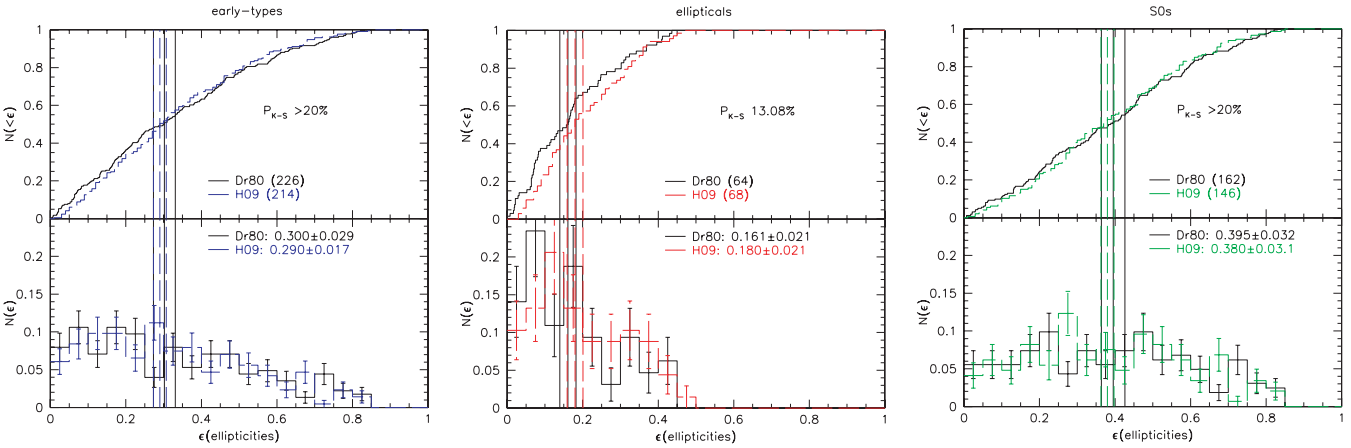

Figure 15. Comparison between the distribution of WINGS ellipticities for galaxies that are early types for Dressler (1980) (black solid lines) and the low-z sample of Holden et al. (2009). Top panels: cumulative distributions; bottom panels: histograms normalized to 1. P_{K-S} is the probability of the two distributions drawn from the same parent distribution. Left-hand panel: comparison between WINGS and Holden et al. (2009) (blue dashed lines) early types. Middle panel: comparison between WINGS and Holden et al. (2009) (red dashed lines) ellipticals. Right-hand panel: comparison between WINGS and Holden et al. (2009) (green dashed lines) S0s.

This is consistent with the assumption that Holden et al. (2009) estimates of the galaxy ellipticity are compatible with ours.

Secondly, we check that using only WINGS clusters also classified by Dressler is equivalent to using the whole WINGS data set: in fact the ellipticity distributions for WINGS clusters in common with Dressler (1980) (18 clusters) are in agreement with that of our whole sample (76 clusters) (plots not shown, $P_{K-S} \gg 20$ per cent for all the morphological types). The three distributions (early types, ellipticals and S0s) are very similar, indicating that the WINGS clusters in common with Dressler (1980) are not a biased subsample of the whole WINGS data set.

Since ellipticity measurements do not seem to be responsible for the differences between the two data sets, we focus our attention on the other possible sources of differences, starting with the morphological classifications.

We find that ∼27 per cent (79/296) of the galaxies have been classified differently from us and Dressler (1980). This corresponds to the typical agreement between independent classifiers (see also Section 2.1). However, we have checked that they are too few to influence the overall ellipticity distribution. Even by reclassifying them and moving them to the other morphological class they do not alter the ellipticity distribution of the class in which they have been inserted.

Moreover, comparing the ellipticity distribution of galaxies belonging to the same morphological class for us and for Dressler (1980), once again we find no significant differences (the K–S test is always largely inconclusive) (plots not shown).

So, the inconsistency is not even linked to the different morphological classification and we have to focus on possible biases due to other factors.

Thirdly, we investigate the magnitude distributions of Holden et al. (2009) and WINGS samples to be sure that all samples are equally deep. In Fig. 16, we compare the magnitude distribution of the analysed samples and we find that the magnitude distribution of the subsample of galaxies with Dressler (1980) morphologies (therefore those used by Holden et al. 2009) (red filled histogram)

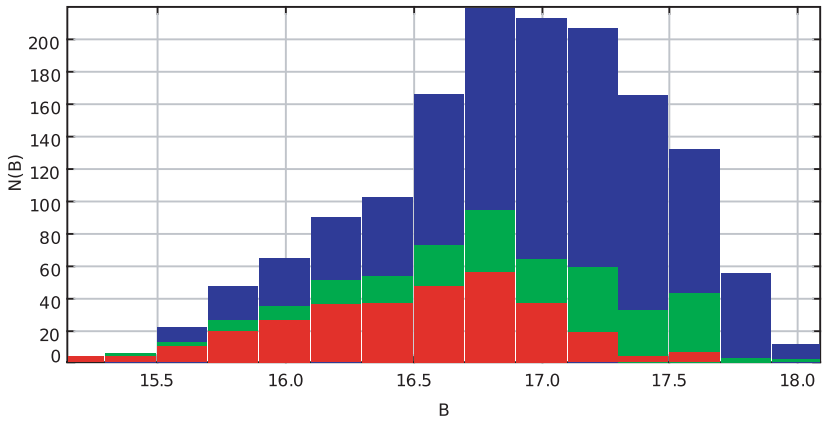

Figure 16. Magnitude distribution of galaxies in different samples. Blue histogram: early-type galaxies in the whole WINGS sample (1494 galaxies). Green histogram: early-type galaxies in the WINGS subsample of clusters that are in common with Dressler's (1980) (547 galaxies). Red histogram: galaxies early types in the WINGS sample that are in common with Dressler's (1980) (296 galaxies).

is very different from that of our galaxies, both if we consider only the clusters that are in common (green filled histogram) and if we consider the whole WINGS sample (blue filled histogram). Performing a K–S test on the magnitude distributions, we find that the whole WINGS sample and the subsample of galaxies with Dressler (1980) morphologies are drawn from different parent distributions ($P_{\rm K-S} = 2$ per cent). Since we are following exactly the same selection criteria, the magnitude distributions should have been similar. It seems that the Dressler (1980), and hence the Holden et al. (2009), low-z sample misses galaxies at fainter magnitudes. Probably they are too faint to have been morphologically classified by Dressler (1980) who used photographic plates for the classification.

To test whether this bias considerably alters the ellipticity distribution, we create magnitude-matched samples, selecting from our WINGS sample a subsample of galaxies with the same magnitude (within ± 0.05 mag), the same morphology and in the same cluster as the sample of Dressler (1980) used by Holden et al. (2009). As shown in Fig. 17, comparing the WINGS magnitude-matched simulated sample with the Dressler (hence Holden et al. 2009) sample, the ellipticity distributions are compatible for early-types, ellipticals and S0s (the K–S test cannot reject the null hypothesis of a common origin of the distribution, giving a probability always >20 per cent).

We conclude that the differences observed between the WINGS and the Holden samples in the local Universe are due to the fact that the latter includes only those galaxies that were morphologically classified by Dressler (1980) and do not correspond to a complete sample within the adopted magnitude limits. Therefore, when comparing the WINGS and the low-z Holden et al. (2009) sample, we are not comparing samples with the same properties, that is, with the same magnitude distribution.

5.1.2 *EDisCS and Holden et al. (2009)*

Now we wish to check if there are some differences also between the EDisCS and the Holden et al. (2009) sample.

Having the ellipticities of both samples, we can compare directly the ellipticity distributions of the two samples at high z. Fig. 18 shows the comparison between the EDisCS and Holden et al. high-z ellipticity distributions for the different morphological types. We find that there are no significant differences ($P_{\rm K-S} \sim 11$, ≥ 20 and ≥ 20 per cent for early types, ellipticals and S0s, respectively). Also comparing the ellipticity distribution of galaxies belonging only to the clusters in common (plots not shown), we can state that there are no discrepancies between the samples, as the K–S test is always largely inconclusive ($P_{\rm K-S}$ always $\gg 20$ per cent).

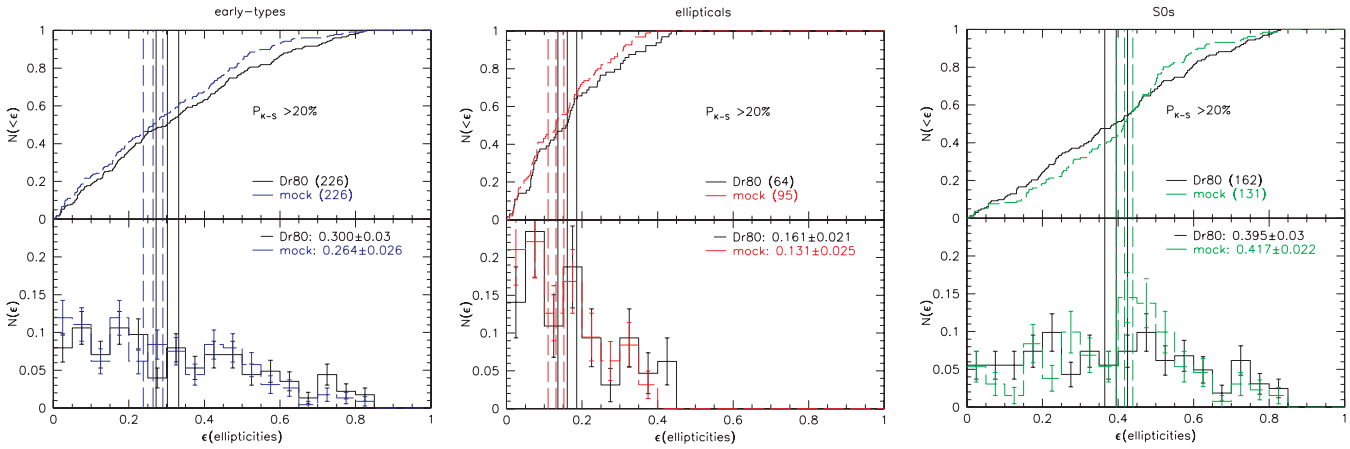

Figure 17. Ellipticity distribution of magnitude-matched samples (see text for details) for early types (left-hand panel), ellipticals (middle panel) and S0s (right-hand panel). Panels and symbols are as usual. Black solid lines represent WINGS galaxies present in the Dressler (1980) catalogue; coloured dashed lines represent WINGS mock distributions.

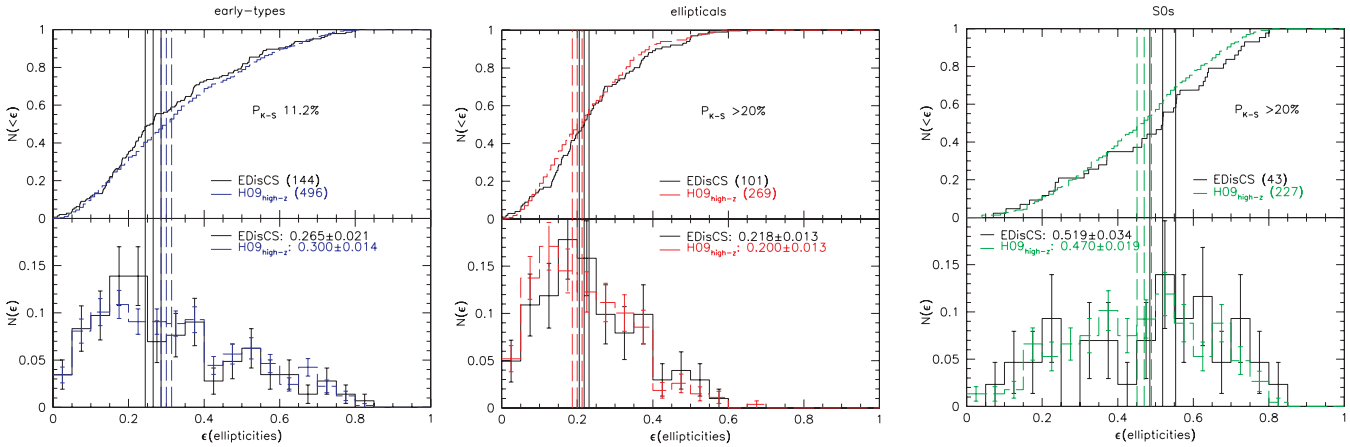

Figure 18. Comparison between our results and those of Holden et al. (2009) at high z. All clusters are used in both samples. Top panels: cumulative distributions; bottom panels: histograms normalized to 1. P_{K-S} is the probability of the two distributions drawn from the same parent distribution. Left-hand panel: comparison between EDisCS (black solid lines) and Holden et al. (2009) (blue dashed lines) early types. Middle panel: comparison between EDisCS (black solid lines) and Holden et al. (2009) (red dashed lines) ellipticals. Right-hand panel: comparison between EDisCS (black solid lines) and Holden et al. (2009) (green dashed lines) S0s.

5.2 Conclusions

To conclude, the different results drawn by analysing our samples and that of Holden et al. (2009) mainly arise from the fact that, despite the fact that, in principle, galaxies are selected following the same criteria, actually at low z they have a different magnitude distribution. The Holden et al. (2009) low-z sample suffers from incompleteness at faint magnitudes, likely due to the lack of availability of Dressler (1980) morphologies at faint magnitudes. No differences have been detected instead at high z between Holden et al.'s sample and ours.

6 SUMMARY AND CONCLUSIONS

In this paper, we have analysed the ellipticity distribution of early-type galaxies, and of ellipticals and S0s separately, in clusters at $z =$ 0.04–0.07 and 0.4–0.8. We have taken into account both a mass-limited sample and a magnitude-'delimited' sample of galaxies.

(i) In our mass-limited samples, above the common mass limit ($M_* \geq 10^{10.2}\,M_\odot$) the ellipticity distribution of early-type galaxies strongly varies with redshift. This is due to a change in both the median and the shape of the distributions with redshift. For ellipticals, no statistically significant differences are observed in the high- and low-z distribution, even if an evolution of the medians is detected and we observe an excess population of round ellipticals at low z compared to high z. Finally, no evolution is observed for S0s. The evolution of early-type galaxies is not simply related to the different mass distributions at high z and low z. In fact, removing the influence of the mass, the results remain inconsistent. Instead, it is mainly related to the evolution of the morphological mix with redshift and hence to the relative contribution of ellipticals and S0s at the two epochs.

(ii) As mentioned in the previous point, in our low-z sample, we find a population of very round ($\epsilon \leq 0.05$) elliptical galaxies that is less conspicuous at high z. This population seems real and not due to selection effects or measurement problems.

(iii) In our magnitude-'delimited' sample, for early types and S0s, the evolution is not evident (though the medians of both early types and S0s change with z), while for ellipticals, we have found a change in the distribution with redshift.

(iv) The observed differences between the mass-limited sample and the magnitude-'delimited' one can be due to the different mass distribution of the two samples: in fact in the magnitude-'delimited' samples, we are loosing some galaxies that enter the mass-limited one, both at high and, especially and more importantly, at low masses.

(v) Our magnitude-'delimited' results are not in agreement with those of Holden et al. (2009), who also analysed a magnitude-'delimited' sample of early types belonging to the red sequence. The main reason of the observed discrepancy is that, despite galaxies being selected following, in principle, the same criteria, in practice the two low-$z$samples have a different magnitude distribution because the Holden et al. (2009) sample suffers from incompleteness at faint magnitudes.

ACKNOWLEDGMENTS

We want to thank B. P. Holden for providing us the lists of ellipticities from his paper. We thank G. Rudnick for his useful comments that improved our paper. We also thank the anonymous referee for their help in making our paper more readable. BV and BMP acknowledge financial support from ASI contract I/016/07/0.

REFERENCES

Bell E. F., de Jong R. S., 2001, ApJ, 550, 212
Bertin E., Arnouts S., 1996, A&AS, 117, 393
Bertola F., Capaccioli M., 1975, ApJ, 200, 439
Blakeslee J. P. et al., 2006, ApJ, 644, 30
Blanton M. R., Roweis S., 2007, AJ, 133, 734
Bolzonella M., Miralles J.-M., Pelló R., 2000, A&A, 363, 476
Brinchmann J., Charlot S., White S. D. M., Tremonti C., Kauffmann G., Heckman T., Brinkmann J., 2004, MNRAS, 351, 1151
Brunner R. J., Lubin L. M., 2000, AJ, 120, 2851
Cappellari M. et al., 2005, Nearly Normal Galaxies in a LCDM Universe. UC Santa Cruz, Santa Cruz
Cava A. et al., 2009, A&A, 495, 707
Conselice C. J., 2003, ApJS, 147, 1
Conselice C. J., Bershady M. A., Jangren A., 2000, ApJ, 529, 886
De Lucia G. et al., 2004, ApJ, 610, L77

De Lucia G. et al., 2007, MNRAS, 374, 809
de Vaucouleurs G., de Vaucouleurs A., Corwin H. G., Jr, Buta R. J., Paturel G., Fouqué P., 1991, Third Reference Catalogue of Bright Galaxies, Volume 1-3, XII, 2069. Springer-Verlag, Berlin, Heidelberg, New York
Desai V. et al., 2007, ApJ, 660, 1151
Dressler A., 1980, ApJ, 236, 351
Dressler A. et al., 1997, ApJ, 490, 577
Ebeling H., Voges W., Bohringer H., Edge A. C., Huchra J. P., Briel U. G., 1996, MNRAS, 281, 799
Ebeling H., Edge A. C., Bohringer H., Allen S. W., Crawford C. S., Fabian A. C., Voges W., Huchra J. P., 1998, MNRAS, 301, 881
Ebeling H., Edge A. C., Allen S. W., Crawford C. S., Fabian A. C., Huchra J. P., 2000, MNRAS, 318, 333
Erwin P., Beltrán J. C. V., Graham A. W., Beckman J. E., 2003, ApJ, 597, 929
Fasano G., Poggianti B. M., Couch W. J., Bettoni D., Kjærgaard P., Moles M., 2000, ApJ, 542, 673
Fasano G. et al., 2006, A&A, 445, 805
Fasano G. et al., 2007, in Vallenari A., Tantalo R., Portinari L., Moretti A., eds, ASP Conf. Ser. Vol. 374, From Stars to Galaxies: Building the Pieces to Build Up the Universe. Astron. Soc. Pac., San Francisco, p. 495
Fasano G. et al., 2010, MNRAS, 404, 1490
Fritz J. et al., 2007, A&A, 470, 137
Fritz J. et al., 2010, A&A, 526, A45
Gehrels N., 1986, ApJ, 303, 336
Gonzalez A. H., Zaritsky D., Dalcanton J. J., Nelson A., 2001, ApJS, 137, 117
Halliday C. et al., 2004, A&A, 427, 397
Holden B. P. et al., 2009, ApJ, 693, 617
Hubble E. P., 1936, Realm of the Nebulae. Yale University Press, New Haven
Kauffmann G., et al., 2003, MNRAS, 341, 54
Kroupa P., 2001, MNRAS, 322, 231
Laurikainen E., Salo H., Buta R., Knapen J. H., 2007, MNRAS, 381, 401
Lotz J. M., Primack J., Madau P., 2004, AJ, 128, 163
Mann H. B., Whitney D. R., 1947, Ann. Math. Stat., 18, 50
Marleau F. R., Simard L., 1998, ApJ, 507, 585
Mei S. et al., 2009, ApJ, 690, 42
Milvang-Jensen B. et al., 2008, A&A, 482, 419
Moses L. E., 1963, Ann. Math. Stat., 34, 973
Pelló R. et al., 2009, A&A, 508, 1173
Peng C. Y., Ho L. C., Impey C. D., Rix H.-W., 2002, AJ, 124, 266
Pignatelli E., Fasano G., Cassata P., 2006, A&A, 446, 373
Poggianti B. M., 1997, A&AS, 122, 399
Poggianti B. M. et al., 2006, ApJ, 642, 188
Poggianti B. M. et al., 2008, ApJ, 684, 888
Postman M. et al., 2005, ApJ, 623, 721
Rood H. J., Baum W. A., 1967, AJ, 72, 398
Rudnick G. et al., 2001, AJ, 122, 2205
Rudnick G. et al., 2003, ApJ, 599, 847
Rudnick G. et al., 2006, ApJ, 650, 624
Rudnick G. et al., 2009, ApJ, 700, 1559
Salpeter E. E., 1955, ApJ, 121, 161
Sandage A., Freeman K. C., Stokes N. R., 1970, ApJ, 160, 831
Scorza C., van den Bosch F. C., 1998, MNRAS, 300, 469
Simard L. et al., 2002, ApJS, 142, 1
Simard L. et al., 2009, A&A, 508, 1141
Tran K.-V. H., van Dokkum P., Franx M., Illingworth G. D., Kelson D. D., Schreiber N. M. F., 2005, ApJ, 627, L25
Valentinuzzi T. et al., 2009, A&A, 501, 851
Valentinuzzi T. et al., 2010, ApJ, 712, 226
van Dokkum P. G., Franx M., Fabricant D., Kelson D. D., Illingworth G. D., 1999, ApJ, 520, L95
Varela J. et al., 2009, A&A, 497, 667
Vulcani B. et al., 2010a, MNRAS, preprint (arXiv:1010.4442)
Vulcani B., Poggianti B. M., Finn A., Rudnick G., Desai V., Barnford S., 2010b, ApJ, 710, L1
White S. D. M. et al., 2005, A&A, 444, 365
Wilman D. J., Oemler A., Mulchaey J. S., McGee S. L., Balogh M. L., Bower R. G., 2009, ApJ, 692, 298

APPENDIX A: ADDITIONAL STATISTICAL TESTS

In Section 3.2, we characterize the evolution of the ellipticity distribution by performing the K–S test. Anyway, since this test is as general as possible, we wish to go deeper into our analysis, trying to understand if the K–S results are confirmed and above all if they are driven by a different shape of the distributions or simply by a different location of the two populations. To do this, we perform two other statistical non-parametric tests (i.e. they do not assume the normal distribution) which make no assumptions about the distributions of the populations.

We use the Moses (1963) test to check the equality of the scale parameter, taking into account that each population has a different median. This test is very useful to compare the shape of two distributions and to evaluate their dispersion. Following this procedure, we subdivide each population into a certain number of groups, each one containing 10 observations. For each group, we compute its average and the sum of the residuals. Then we put together all the residuals of the two populations, paying no attention which one each value belongs to, and we sort them. Afterwards, we sum the rank of each population separately and we compare the sums. If they are very different, the probability that the populations are drawn from the same parent distribution is very small. Since this test requires to consider randomly a subsample of the observations of the populations, we repeat the test 1000 times.[10] It emerges that early-type galaxies at different redshifts are unlikely to have the same scale parameter (with a probability <5 per cent in 85 per cent of the simulations), while both ellipticals and S0s show a high compatibility of it (with a probability <5 per cent only in 14 per cent of the simulations in both cases), suggesting that the shapes of the distributions are similar at different redshifts.

Then, to test if there could be a shift in the location between the populations, we adopt the U-statistic proposed by Mann & Whitney (1947). This allows us to assess if there are differences in the median values, regardless of the choice of the errors adopted to characterize the medians. This procedure requires to rank all the values, without regards to which population each value belongs to.[11] Similarly to what we did for the Moses test, we sum the ranks of each population and we compare the sums. Again, if they are very different, the hypothesis that the two populations are drawn from the same parent distribution is ruled out. This test strongly supports the hypothesis that early types and ellipticals have a different median at different redshifts, while for S0s, it cannot exclude the similarity of them (giving, respectively, a probability of 0.06, 1.17 and 17.12 per cent, respectively). We note that these results are fully in agreement with the bootstrap errors (see Table 5).

A detailed summary and comparison of the results of the different tests is shown in Table 9, both for the mass-limited sample and the magnitude-'delimited' one.

[10] Since this test is based on random samples, we do not take into account the WINGS' weights.

[11] To take into account the WINGS' incompleteness, here we consider rounded WINGS' weights, so that WINGS galaxies can weigh 1, 2 or 3, according to their real weight.

Table A1. Summary of the results of different tests applied both to our mass- and to our magnitude-'delimited' samples (see Section 4). The K–S test, being as general as possible, gives an indication on whether the two distributions can derive from the same parent distribution; the Moses test examines the equality of scale parameters when the assumption of common medians is not reasonable (hence, it tests the *shape*); the Mann–Whitney test examines if there is a shift in the median of the two populations (hence, it tests the compatibility of the *medians*). For the mass-limited sample, only galaxies above $\log M/\mathrm{M}_{\odot} \geq 10.2$ are considered. Moreover, for the WINGS, we also take into account the completeness weights (see text for details). The symbol $\neq$ means that the considered test can state that the two populations are drawn from different parent distributions, while the symbol $=$ means that the considered test is inconclusive.

Test	Early types			Ellipticals			S0s		
K–S	MASS:	0.04 per cent	$\neq$	MASS:	5.84 per cent	$=$	MASS:	>20 per cent	$=$
	MAG:	7.7 per cent	$=$	MAG:	0.41 per cent	$\neq$	MAG:	11.9 per cent	$=$
Moses	MASS:	<1 per cent in 60 per cent 1–5 per cent in 25 per cent 5–10 per cent in 7 per cent >10 per cent in 8 per cent	$\neq$	MASS:	<1 per cent in 3 per cent 1–5 per cent in 11 per cent 5–10 per cent in 12 per cent >10 per cent in 74 per cent	$=$	MASS:	<1 per cent in 2 per cent 1–5 per cent in 12 per cent 5–10 per cent in 10 per cent >10 per cent in 76 per cent	$=$
	MAG:	<1 per cent in 28 per cent 1–5 per cent in 25 per cent 5–10 per cent in 17 per cent >10 per cent in 30 per cent	$\neq$	MAG:	<1 per cent in 16 per cent 1–5 per cent in 23 per cent 5–10 per cent in 10 per cent >10 per cent in 51 per cent	$=$	MAG:	<1 per cent in 1 per cent 1–5 per cent in 9 per cent 5–10 per cent in 13 per cent >10 per cent in 77 per cent	$=$
Mann–Whitney	MASS:	0.06 per cent	$\neq$	MASS:	1.17 per cent	$\neq$	MASS:	17.12 per cent	$=$
	MAG:	13.18 per cent	$=$	MAG:	0.07 per cent	$\neq$	MAG:	3.4 per cent	$\neq$

APPENDIX B: HOW CAN RESULTS FROM DIFFERENT SAMPLES BE RECONCILED?

From Sections 3 and 4 we draw different results. Summarizing, we have found that in our mass-limited sample, there is no clear trend between the ellipticity and mass for S0s. For ellipticals, this trend is only hinted, with more massive galaxies having slightly lower values of ellipticity, while for early types, it is quite strong and mostly due to the fact that ellipticals and S0s are found in different proportions at different masses.

Comparing the ellipticity distributions at the two redshifts, we have found an evolution for the early types, with WINGS galaxies being proportionally more flattened than EDisCS galaxies. No strong evolution has been detected for ellipticals and S0s separately, except for the likely presence of an enhanced population of round ellipticals at low z. Note that this trend for round ellipticals is *opposite* to the trend for all early-type galaxies (rounder versus flatter at low z, respectively); therefore, we must be observing two distinct evolutionary effects.

In contrast, from the analysis of the magnitude-'delimited' sample, we cannot exclude that, both in the case of early-type galaxies and in the case of S0s, the galaxy samples at high z and low z are drawn from the same parent distribution, although the change in the median ellipticity values with time seems to indicate an evolution instead. Moreover, we have found a significant evolution (2σ error) of the ellipticity distribution of elliptical galaxies, due mainly to a different median of the distributions.

To understand the reasons for the observed discrepancies, we have compared directly the ellipticity distributions of the mass-limited and magnitude-'delimited' samples for the same type of galaxies at the same redshift (plots not shown).

The K–S test suggests different distributions ($P_{\mathrm{K-S}} \sim 0$ per cent) for WINGS early types and S0s, while it is inconclusive in all other cases (i.e. WINGS ellipticals; EDisCS early types, ellipticals and S0s, $P_{\mathrm{K-S}} \gg 20$ per cent). Going deeper into the analysis, WINGS early types show incompatible values both of the median (the Mann–Whitney test gives a probability of 0.90 per cent) and of the scale parameter (the Moses test gives a probability <5 per cent in 80 per cent of the simulations), while WINGS S0s have different scale parameters (the Moses test gives a probability <5 per cent in 83 per cent of the simulations).

The origin of the observed differences in the distributions probably lies in the fact that galaxies in the two samples are characterized by different properties; in particular, in the magnitude-'delimited' samples, selecting galaxies only in the magnitude range $-19.3 > M_B + 1.208z > -21$, we are loosing (the few) most-massive galaxies and a large fraction of the less-massive galaxies.

This is evident in Fig. 19, where we compare the galaxy stellar mass functions of our mass-limited and magnitude-(de)limited samples, as derived in Vulcani et al. (2010a). It is clear that the magnitude-'delimited' sample is incomplete at low and at high masses, and much more so for S0s at low masses in the local Universe than at high z.

The net effect of the differential incompleteness in mass at high z and low z in magnitude-selected samples is to artificially deprive the low-z distribution preferentially of high-ellipticity (S0) galaxies. The loss of low-mass S0s (more flattened) at low z greatly reduces the differences between the high- and low-z ellipticity distribution of early-type galaxies, bringing their medians to be almost consistent and the K–S test to be inconclusive.

For ellipticals, the net effect of the incompleteness of the magnitude-'delimited' sample is to exacerbate the differences with redshift, again subtracting low-mass (hence higher ellipticity) ellipticals at low z.

The incompleteness in the mass distributions of the magnitude-'delimited' sample therefore seems to be consistent with the differences we observe between the ellipticity distributions of the mass-limited and magnitude-'delimited' samples. The magnitude-'delimited'sample is biased; in particular, early-type galaxies on the red sequence and with $-19.3 > M_B + 1.208z > -21$ are not representative of the overall population.

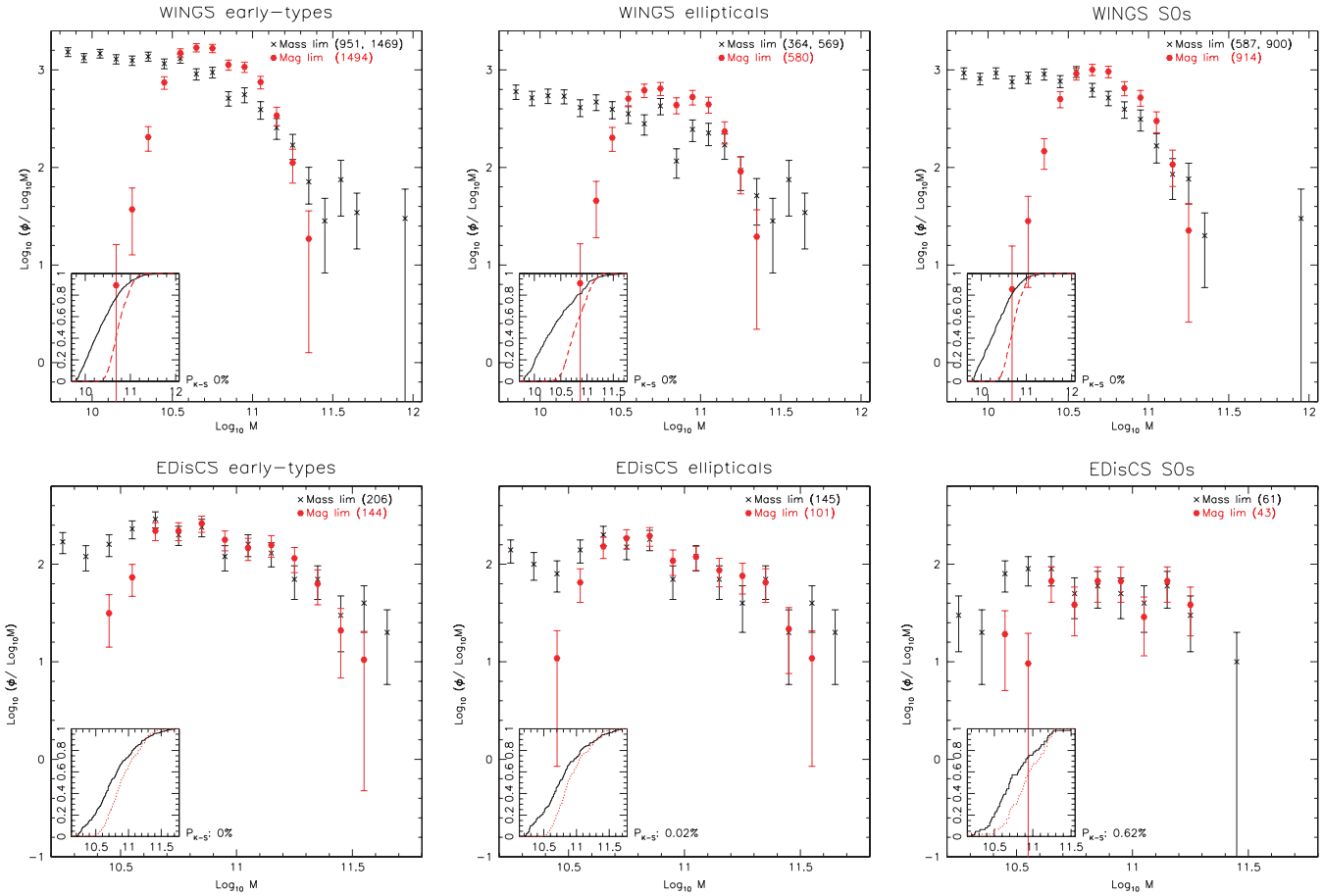

Figure 19. Comparison between the mass functions of the mass-limited (black crosses) and the magnitude-(de)limited (red points) samples for WINGS (upper panels) and EDisCS (bottom panels) early types, ellipticals and S0s.

This paper has been typeset from a TEX/LATEX file prepared by the author.